BSPE 97679-00-1113-7

지구화학적 추적자를 이용한 고기후 연구

Paleoclimate Reconstruction Using Geochemical Tracers

1998. 12.

해 양 수 산 부
한 국 해 양 연 구 소

제 출 문

해양연구소 소장 귀하

본 보고서를 "지구화학적 추적자를 이용한 고기후 연구" 보고서로 제출합니다.

1998년 12월

한국해양연구소

연구책임자 : 박병권

연 구 원 : 윤호일

김동선

이보화

요 약 문

1. 제 목

지구화학적 추적자를 이용한 고기후 연구

2. 연구개발의 목적 및 중요성

20세기 이후 급속한 산업화로 인하여 석유, 석탄, 천연가스 등 화석 연료의 사용이 급격히 증가함으로서 엄청난 양의 이산화탄소가 대기 중으로 방출되어지고 있다 대기 중 이산화탄소 농도 증가는 온실효과를 통해 대기 온도를 증가시키기 때문에 인류의 생존에 직접적으로 영향을 미치고 있다. 이처럼 인류의 생존에 직접적으로 영향을 미치는 미래 기후변화를 예측하기 위해서는 과거 기후변화를 정확히 이해하는 것이 필요하다.

3. 연구개발의 내용 및 범위

가. 남극 킹조지섬 맥스웰만에서 지난 빙하기 이후 유공충과 방해석 용존에 대한 연구

나. 남극 드랜스필드 해협 퇴적물에서 탄소, 규소, 인에 대한 지화학적 연구

다. 동지나해 북 대륙붕에서 빙하기 이후 고해양학적 기록에 대한 연구

4. 연구개발 결과

가. 남극 킹조지섬 맥스웰 만은 지난 빙하기동안 해빙에 의해 완전히 덮혀 있어서 일차생산성이 거의 일어나지 않아 퇴적물속의 유기물과 유공충 함량이 낮았다. 반면에 빙하기 이후에 일차생산성이 높아지면서 유기물 공급이 많아져 유공충 함량이 증가하였다.

나. 남극 브랜스필드 해협 퇴적물에서 유기탄소와 생물기원 규소가 퇴적물 깊이에 따라 주기적인 변화를 보이는데 이것은 표층해수에서 일차생산성이 주기적으로 변하였기 때문이다. 또한 이런 일차생산성의 주기적인 변화는 과거 수천년전 이 지역에서 기후도 주기적으로 변하였다는 것을 의미한다

다. 유공충 연구 결과에 의하면 동지나해 북 대륙붕 지역은 빙하기 동안에 연안해수 영향을 많이 받았고 빙하기가 끝날 무렵에는 황해냉수에 의해 영향을 받았다. 그리고 만년 전에는 황해난류가 우세하였고 7500년 전 이후에는 쿠류시오 해류의 영향을 많이 받았다

SUMMARY

1. Title

Paleoclimate reconstruction using geochemical tracers

2. Significance and Goal of the study

Huge amounts of anthropogenic carbon dioxide have emitted by use of fossil fuels, such as petroleum, coal, and natural gas since 20 century. The increase of carbon dioxide causes global warming through the green house effect, which threatens the human life in near-future. In order to predict climatic changes in near-future that affects directly human life, therefore, we must figure out the paleoclimatic changes during the late Holocene.

3. Contents and Scope of the Study

a. Foraminiferal assemblage and $CaCO_3$ dissolution since the last deglaciation in the Maxwell Bay, King George Island, Antarctica

b. Geochemistry of carbon, silica, sulfur, and phosphorus in the Bransfield Strait sediments, Antarctica

c. Paleoceanographic records from the northern shelf of the East China Sea after the Last Glacial Maximum

4. Result of the Study

a. During the last glaciation, extensive sea ice prevented the production of primary organisms in the Maxwell Bay, King George Island, Antarctica, so there was a low TOC and foraminiferal abundance in the sediment; while after the glacial, higher flux of organic carbon from the higher primary productivity caused the foraminiferal proliferation.

b. In the Bransfield Strait sediments, organic carbon and biogenic silica show cyclical downcore variations, which are mostly caused by periodic productivity changes in the water column over times. The periodic productivity changes imply that the climate in the Brasfield Strait has cyclically changed during the last several thousand years.

c. The foraminiferal fauna disclose the water mass history in the northern shelf of the East China Sea. During the last glacial, the dominate water might be the coastal water; and at the end of the last glacial, the Yellow Sea cold water mostly affected this area. Then it gave way to the Yellow Sea Warm Current after 10,000 yr B.P. and finally the warm water dominated this area after 7,500 yr B.P., due to enhancement of the Kuroshio Current.

목차

LIST OF FIGURES

LIST OF TABLES

제 1 장 서 론

19세기 이후 급속한 산업화로 인한 화석연료 사용 증가는 엄청난 양의 이산화탄소를 대기 중으로 방출시키고 있다. 대기 중 이산화탄소 농도 증가는 온실효과를 유발시켜 지구환경 변화에 직접적인 영향을 미치고 있다. 이산화탄소 농도가 현재와 같은 추세로 증가한다면 2050년에는 그 농도가 현재의 2배가 되고 지구 평균 온도가 2 – 3 ℃ 가량 증가한다고 예측하였다. 이런 온도 증가는 대규모 태풍의 발생, 지구의 사막화, 해빙에 따른 해수면 상승, 병충해의 발생 등 여러 가지 재앙을 일으켜서 인류의 생존을 위협한다. 이런 까닭에 현재 세계 각국은 막대한 예산을 투자하여 대기중 이산화탄소 농도 변화와 동태 및 지구환경에 미치는 영향을 수행하고 있다. 그 일환으로 Joint Global Ocean Flux Study (JGOFS)와 같은 연구 프로그램을 통하여 대기에서 해양으로 유입되는 이산화탄소의 동태를 연구하고 있다 또한, Past Global Changes (PAGE) 와 같은 공동연구 프로그램을 통하여 과거의 지구환경 변화를 연구함으로써 미래의 지구환경 변화를 예측하려는 연구가 지속적으로 진행되고 있다.

과거 기후변화는 빙하기와 간빙기가 반복적으로 나타나는 장기간 변화와 빙하기 또는 간빙기 동안에 나타나는 단기간 변화로 나누어 진다. 현재까지 빙하기와 간빙기가 반복적으로 나타나는 장기간 변화는 많은 연구가 이루어져 정확히 그 주기와 시간을 예측되지만 빙하기 또는 간빙가 동안에 나타나는 단기간 변화에 대해서는 그 주기와 시간 뿐 만 아니라 그 이유에 대해서도 아직 밝혀지지 않았다. 15세기에는 전세계적으로 기후가 추워졌던 리틀 아이스 시기(Little Ice Age)가 있었고 10세기에는 갑자기 기후가 따뜻해졌던 시기가 있었다. 이처럼 과거 천년 동안에도 갑작스러운 기후변화가 일어났지만 아직도 연구가 미흡한 형편이다. 과거 만년 즉, 홀로세 동안의 갑작스러운 기후변화를 연구하여 그 이유를 밝히는 것은 미래

기후변화를 예측하기 위해서는 필수적이다.

본 연구에서는 남극 브랜스필드 해협과 맥스웰 만에서 유공충과 지화학적 분석을 통해 과거 만년 동안에 일어났던 해양환경 변화 및 기후 변화를 밝힐려고 한다. 그리고 동지나해 북 대륙붕에서 수직적인 유공충 조합의 변화를 통해 지난 빙하기와 간빙기 동안 기후 변화에 직접적인 영향을 미치는 해양 수괴의 변화를 알아보려고 한다.

제 2 장 남극 킹조지섬 맥스웰만에서 지난 빙하기 이후 유공충과 방해석 용존에 대한 연구

Chapter 2 Foraminiferal assemblage and $CaCO_3$ dissolution since the last deglaciation in the Maxwell Bay, King George Island, Antarctica

2-1. Abstract

Down-core variation of carbonate dissolution index and the comparison among gravity cores of different water depths from the Maxwell Bay, King George Island, Antarctica indicated that the water masses is one of the most important factors controlling the distribution of benthic foraminifera during the glacial marine environment. We suggest that tha dissolution of carbonate and foraminifera shell is affected by the shallow CCD connected to the water masses in this area. The less influence of the Saline Shelf Water during tha last deglaciation gave the carbonate a well-preservation; with the sea-level increasing and retreat of coastal ice after the glacial, the erosive water mass and the higher CO_2 accumulated by more organic material led to a serious dissolution of $CaCO_3$ and foraminiferal shell in the sediments.

The contrast of water surface environment between the last glaciation and post glacial causes the variation of benthic foraminiferal abundance by the surface primary productivity and tha relevant flux of organic carbon in to the marine bottom. During the last glaciation, extensive sea ice prevented the production of primary organisms, so there was a low TOC and foraminiferal abundance in the sediment; while after the glacial, higher flux of organic carbon

from the higher primary productivity caused the foraminiferal proliferation.

2-2. Introduction

The Antarctic continent and its surrounding south Ocean represent one of the major climate engines of the earth. The dynamic changes of Antarctic environment have play a key role in long term global paleoenvironmental evolution (Kennett & Warnke, 1992).

It was reported that the climate of South Shetland Islands of the northern Antarctica is a relatively warm with high levels of precipitation compared with other parts of the region (Griffith & Anderson, 1989). This modern climate conditions produce a temperate to sub-polar glacial setting which can be sensitive to changes in the environmental factors that influence the advance and retreat of glaciers (Yoon, *et al.*, 1997). For example, quantitative analysis of the numerous lake deposits or fjord sediments have recently disclosed a very frequent records of cold-mild climate variations during the late Holocene (Bjorck *et al.*, 1993, Park *et al.*, 1995).

On the interest of the Glacial history of South Shetland Islands, many different opinions on the Holocene Glacial and environmental changes have been presented with much disagreement. John (1972) and Sugden & Clapperton (1986) got the conclusion that the main deglaciarion of this region occurred before 10,000 BP while Bjorck *et al.*(1991) suggested a main mid-Holocene deglaciation phase in their lake sediment and moss bank studies. Mausbeacher *et al.* (1989) dated the deglaciation of King George Island to 9000-5000 BP based on the bottom sediments of three lakes. Therefore, there exits a series of stages for the last deglaciation: 10,000 BP, 7000 BP, and 6000-5000 BP (Hjort *et al.*, 1992; Inglolfsson *et al.*, 1992).

Most of the paleoceanographic studies on the Antarctic area were conducted in the deep sea basins though they recommended a potential analogue method to shallow waters in discussing the faunal distribution connected with the modern oceanographic characteristics of these deep seas (Kennett, 1966; Berger, 1967; Anderson, 1975a; Osrermna and Kellogg, 1979; Mackensen *et al.*, 1989). However, the changes between Shallow and deep waters have apparently displayed some differences in their paleoceanographic characteristics during the glacial cycles (Anderson, 1975b; Grobe & Mackensen, 1992; Domack & McClennen, 1996); And compared with the lake records, the deep sea sediment from the Antarctica have a low resolution records to recognize the fluctuations of Holocene Paleoceanography, such as in Reddell Sea and Ross Sea. Thus it is very important to get the material in shallow waters which can provide high sedimentary rate, and preserve high-resolution strata.

Recently, much work has been done on the investigation of the geological settings of the shallow water ----Maxwell Bay, including the distributions of minerals, sediments, and microfossils (Li & Zhang, 1986; Chang *et al.*, 1988; Yoon *et al.*, 1992; Yoon *et al.*, 1994; Li & Li, 1996; Woo *et al.*, 1996; Yoon *et al.*, 1997). They have reconstructed some paleoclimate and paleoceanography of late Holocene Antarctica (Chang & Yoon, 1995; Park *et al.*, 1995). However, we still know few about the changes of shallow water properties in the glacial marine environment and its influences on the sediments.

We try to use the marine sediments recently taken from Maxwell Bay, King George Island to add the knowledge of the history of post-glacial climatic and paleoceanographic changes of the shallow waters.

2-3. Material and methods

Three short gravity cores (A10-01, A10-02, and A10-08) were taken by the *R.V.*

Erebus during the expedition of Korea Antarctica Research Program 96/97 from the Marian Cove and Potter Cove, Maxwell Bay, King George Island, Antarctica (Fig. 2-1). The sediments are composed of massive mud, weakly-stratified diamiction, massive clast moderate diamiction or rhythmite (Fig. 2-2). The sample interval is 5-10 cm in three cores, and total 106 samples are analyzed for micropaleontology, sedimentology, geochemistry (Table 2-1).

The weighted dry bulk samples are disaggregated by being soaked in water without adding any chemical agent, then washed through a sieve of 63 μm. The coarse fraction larger than 63 μm was oven-dried and weighted. The foraminiferal specimen are picked up from the coarse fractions.

Foraminiferal and Stable Isotope Analyses

Every foraminiferal specimen is mounted on the paper-made slide, identified, and counted. We follow the standard and descriptions on foraminifera of Crespin (1960), Kennett (1967), Be (1977), Osterman and Kellogg (1979), Setty *et al.* (1980), Finger & Lipps (1981), Milam & Anderson (1981), and Mackensen *et al.* (1990). We identified every specimen, which can be recognized according to their aperture and crust ornaments though sometimes broken (Tables 2-2, 2-3 and 2-4).

After identifying and counting all the individuals, 4-10 foraminiferal specimens from each sample are picked up for stable isotopic analysis. We use benthic species-- *Globocassidulia biora* (or *Globocassidulina crassa rossensis* when the former is too less) to get the values of $\delta^{18}O$ and $\delta^{13}C$. the stable isotopes were analyzed at the Department of Geological Sciences and Marine Science Institute, University of California (Table 2-5).

Analyses of Carbonate and Organic Carbon Contents, C/N ratio and AMS ^{14}C Dating

Total organic carbon (TOC), carbonate contents and C/N ratio were determined using

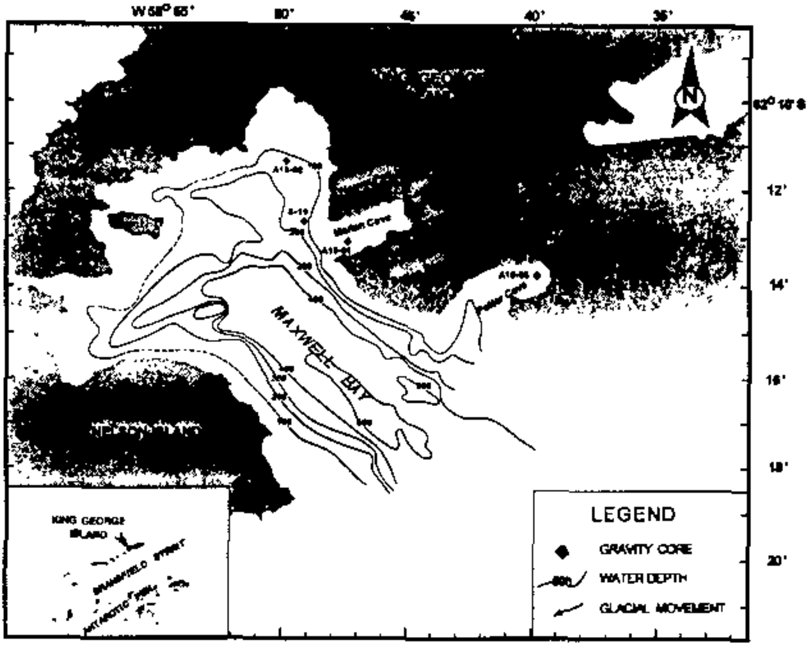

Figure 2-1. Locations of cores A10-01, 02 and 08 in the Maxwell Bay, King George Island, Antarctica

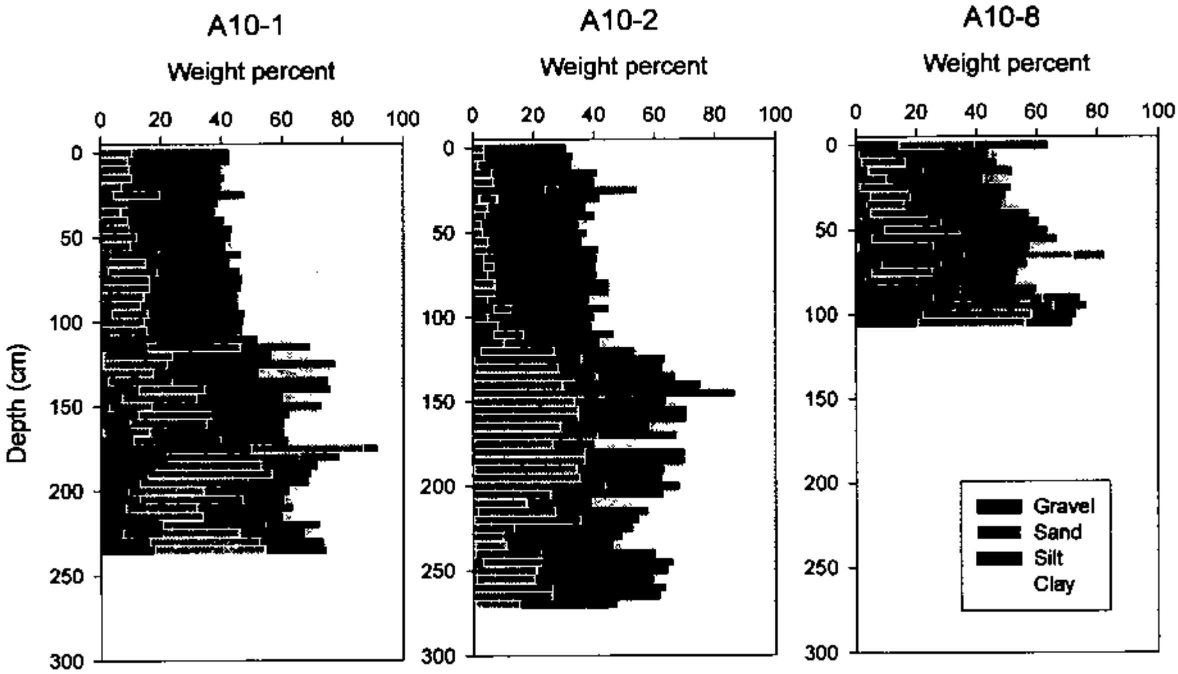

Figure 2-2. Size distribution (content of gravel, sand, silt and cly) in cores A10-01, 02 and 08

Table 2-1. Locations and analyses of three piston cores in the research

Core	Longitude & Latitude	Water depth (m)	Core length (cm)	Foraminifera sample number	$\delta^{18}O$ number	^{14}C date number
A10-01	58°49.7'W 62°11.3'S	110	235	36	10	2
A10-02	58°47.5'W 62°13' S	85	270	49	21	
A10-08	62°39.7'W 62°13.7'S	40	105	21	18	3

Total 5883 specimens analyzed

Table 2-2. Foraminifera species and their relative abundance in Core A10-01

Species	appearance range	average
Globocassidulina biora	(0-100%)	44.9%
Globocassidulina crassa rossensis	(0-100%)	48.6%
Rosalina globularis	(0-8%)	*
Pullenia subcarinata	(0-14%)	*
Astrononion antarcticus	(0-11%)	*
Astrononion echolsi	(0-9%)	*
Miliammina arenacea	(0-33%)	*
Cassidulinoides parkerianus	(0-33%)	*
Cibicides refulgens	(0-15%)	*
Elphidium incertum	(0-8%)	*
Nonionella bradii	(0-40%)	*

* Those species without average percentage values are seldom appearing in the samples

Table 2-3. Foraminifera species and their relative abundance in Core A10-08

Species	abundance	average
Globocassidulina biora	41-95%	76.3%
Globocassidulina crassa rossensis	0-36%	10.2%
Elphidium incertum	0-13%	*
Elphidium sp.1	0-14%	*
Cassidulinoides parkerianus	0-31%	5.4%
Quinqueloculata seminula	0-25%	3.2%
Rosalina globularis	0-1%	*
Astrononion antarcticus	0-1%	*
Pyrgo pentagonica	0-14%	*
Globigerinita glutinata	0-1%	*

* Those species without average percentage values are seldom appearing in the samples.

Table 2-4. Foraminifera species and their relative abundance in Core A10-02

Species	abundance	average
Globocassidulina biora	0-100%	30.4%
Globocassidulina crassa rossensis	0-58%	20.1%
Rosalina globularis	0-2.5%	*
Pullenia subcarinata	0-29%	*
Astrononion echolsi	0-14%	*
Astrononion antarcticus	0-7.1%	*
Miliammina arenacea	0-100%	32.6%
Cassidulinoides parkerianus	0-57%	10.1%
Cassidulinoides porrecta	0-1.6%	*
Cibicides refulgens	0-18%	*
Trifarina angulosa	0-25%	*
Nonionella bradii	0-4.8%	*
Lingulina translucida	0-4.8%	*
Elphidium incertum	0-1.5%	*
Elphidium sp.1	0-2.3%	*
Quinqueloculata seminula	0-0.17%	*
Pyrgo pentagonica	0-1.2%	*
Neogloboquadrina pachyderma L	0-3.0%	*
Globigerinita glutinata	0-1.6%	*

* Those species without average percentage values are seldom appearing in the samples.

Table 2-5. Stable isotope of benthic foraminifera in the three cores

A10-01				A10-02				A10-08			
G.biora		size 0.4-0.7mm		*G.biora*		size: 0.4-0.7mm		*G.biora*		size: 0.4-0.7mm	
Depth (cm)	number	$\delta^{18}O$	$\delta^{13}C$	Depth (cm)	number	$\delta^{18}O$	$\delta^{13}C$	Depth (cm)	number	$\delta^{18}O$	$\delta^{13}C$
10	4	3.828	0.7	0	4	3.786	0.382	0	8	3.837	-0.534
25	7	3.934	0.446	15-20	4	3.811	0.231	5	8	3.851	-0.115
40	2	3.83	0.522	40	4	4.055	0.014	10	10	3.803	-0.124
55	10	3.921	0.717	60	2	3.966	0.75	15	10	3.914	-0.364
60	6	3.78	0.75	70	2	3.992	0.597	20	5	3.773	-0.539
80-95	7	3.786	0.433	105	5	3.841	0.297	25	5	3.885	-1.143
110	8	3.81	-0.057	115-120	7	3.821	0.3	30-35	14	4.04	-1.549
120	6	3.75	0.229	137	4	3.887	-0.164	40	8	3.803	-1.132
145	5	3.86	0.021	160	4	3.747	0.092	45	8	3.872	-1.161
160	3	3.764	0.616	175	6	3.761	0.803	50	10	3.92	-0.399
				189	8	3.785	0.406	55	10	3.875	-0.401
				200	8	3.718	0.24	60	10	3.85	-0.214
				210	4	3.77	0.225	65	8	3.75	-0.148
				220	8	3.833	0.872	70	10	3.97	-1.126
				230	6	3.898	0.505	75	8	3.84	-1.52
				235	9	3.888	-0.118	80	10	3.938	-0.315
				240	10	3.96	0.168	85-90	7	3.971	-0.929
				245	10	3.821	0.191	100-105	7	3.844	-0.551
				255	11	3.872	0.603				
				260-265	17	3.813	0.565				
				270	6	3.847	0.043				

a Carlo-Erba CNS analyzer at the Stable Isotope Laboratory, Polar Research Center of Korea Ocean Research and Development Institute. The material for ^{14}C daring is the organic carbon of bulk sediments The AMS ^{14}C date were measured at Lawrence Livermore National Laboratory, U.S.A. (Table 2-6).

Calculation of Benthic foraminiferal dissolution index (BDI) and Fragmentation

We divided the shell appearance of benthic foraminifera in to three grades: well-preserved (grade 1), common (grade 0) and erosive-affected (grade -1). In the microscope, the well preserved shell (grade 1) shows polished or smooth, opaque appearance while the erosive one (grade -1) display a rough or vague surface. Their shell structure are shown in Fig. 2-3. We counted their number in all the sample and calculate the BDI by using their weighted average. At the same time, we also got the fragmentation by counting the broken shells.

2-4. Results

2-4-1. Stratigraphy

According to the AMS ^{14}C daring, correlation between changes of lithofacies and microfossil fauna in the sediments, we define the strata of three short piston cores from last deglaciation to early Holocene (Fig. 2-4). The main boundary is at depths of 40 cm, 115 cm, and 125 cm in core A10-08, 01, and 02, respectively. The boundary age is about 10,000 cal. yr BP. The lower parts of three cores were the sediment of an ice-proximal environment, composed of coarse diamiction (or rhythmite). While the upper parts of three cores were sediments of ice-distal environment, made up of massive mud. The ages of core-tops are 5508 and 5476 cal. yr BP in A10-08 and A10-01, respectively. Consequently, the sedimentary rate

Table 2-6. Age dating of control point of the Cores

core	depth (cm)	^{14}C age	calendar year (BP)
A10-01	5	5313	5660
	103	8646	9270
	232	13461	15400
A10-08	10	6234	6680
	38.3	9365	9990

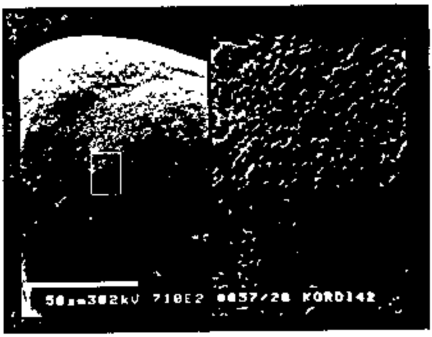

a

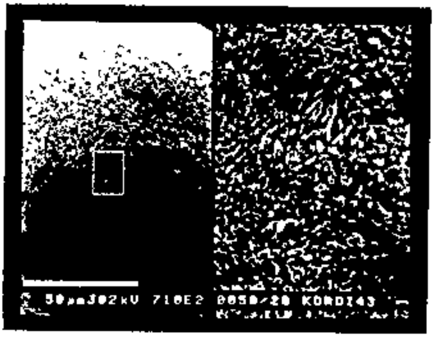

b

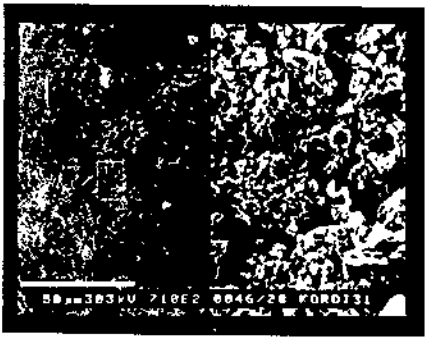

c

d

Figure 2-3. Shell structure of Foraminifera from four depths of Core A10-01

a and b show the surfaces of well-preserved shell in 115 and 230 cm, respectively; c and d show the surface of erosive-affected shell in 15 and 75 cm, respectively.

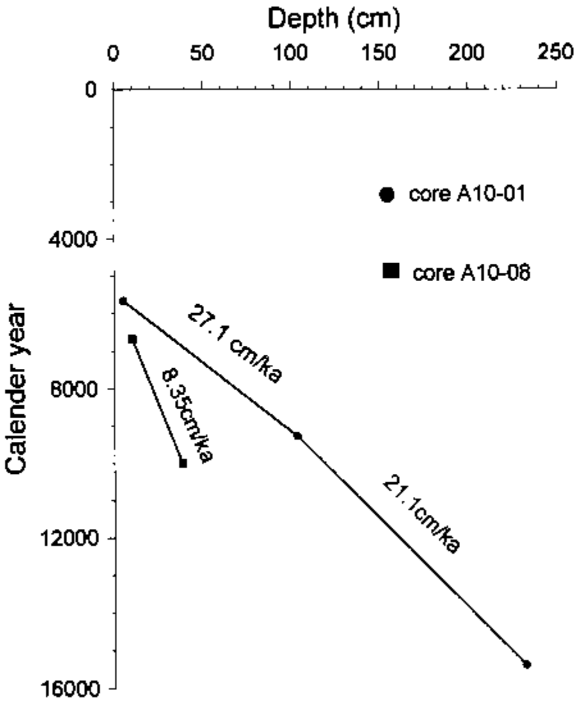

Figure 2-4. Age distribution in cores A10-08 and 01

are 27.1 and 21.1 cm/ka in the upper and lower parts of core A10-01 while core A10-08 have a lower sedimentary rate of 8.53 cm/ka in the upper part. for lack of age dating in core A10-02, we guess that its sedimentary rate are like those of Core A10-01 from the comparison of lithofacies and geochemical data.

All the sediments of three cores were well-preserved except for the interval of 160-270 cm in core A10-02. From the surface appearance of benthic foraminifera in core A10-02 shown in Fig. 2-5, there is a higher percent of yellow shells at the interval of 160-270 cm, so we suggest it might be a kind of redeposit affected by the retreat and advance of ice ground-line at the ice-proximal area during the last deglaciation.

2-4-2. Foraminifera assemblages in three cores

In the samples we examined, 19 benthic and 2 planktonic foraminifera species are recognized (Appendix 2-1). The most abundant species are *Globocassidulina biora*, *Globocassidulina crassa rossensis*, and they sometime account for 50 to 100 percentage of the whole fauna. Another calcareous *Cassidulinoides parkerianus* and an arenaceous *Miliammina arenacea* are the secondary dominant species.

Fig. 2-6 shows the down-core variations of relative abundance of major species in the three cores. The relative abundances of *Globocassidulina biora* have a high value in the lower parts of core A 10-01 and 02, twice the value in the upper parts in average. It seems that the change of *G biora* can be correlated with the variation of coarse fraction (Fig. 2-7): higher percentage of *G. biora* in coarse sediment. *Cassidulinoides perkerianus* have a contrary trend: higher abundances in the upper parts. For example, in depth 10cm of core A10-02, all the specimens are *Ca. perkerianus*.

Core A10-02, the deepest core of the three cores, has a much higher abundance of the arenaceous *Miliammina arenacea* and the foraminiferal fauna sometime consist of only this

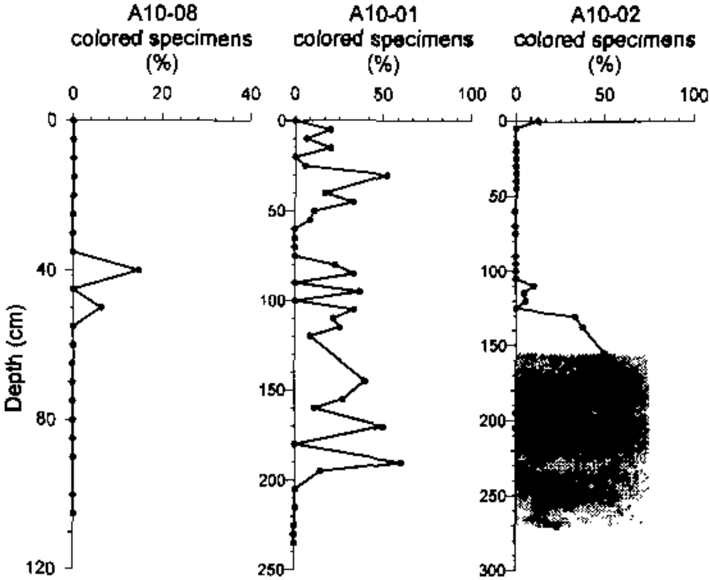

Figure 2-5. Down-core variations of Yellow shell percentage in cores A10-01, 02 and 08

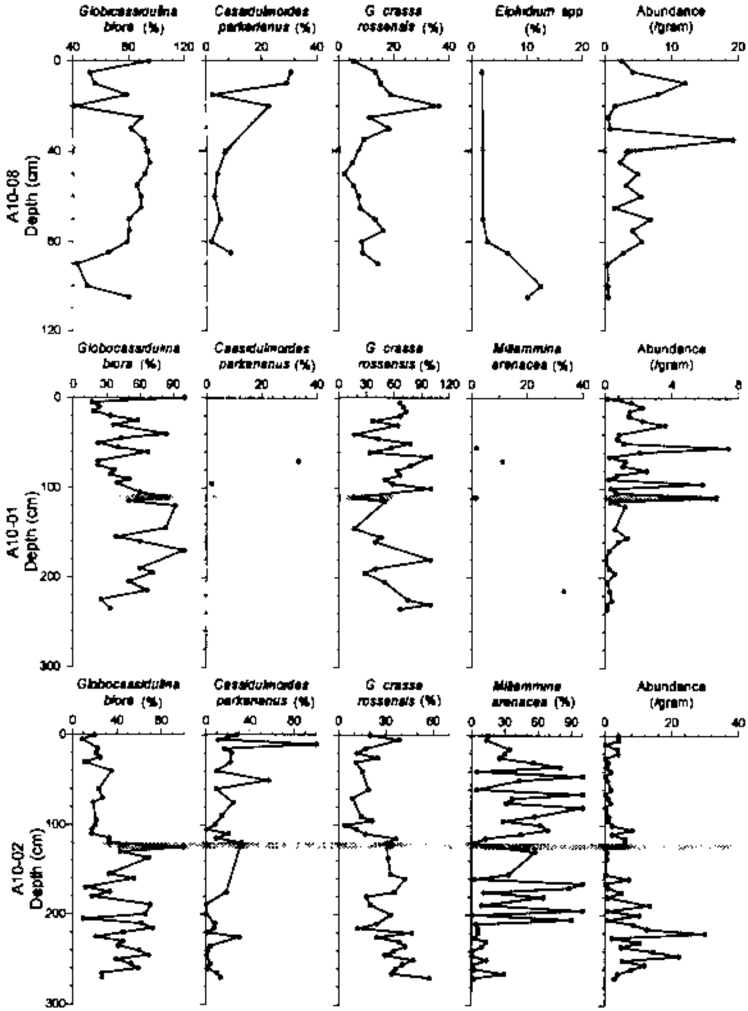

Figure 2-6. Down-core variations of benthic foraminifera and BF abundances in cores A10-01, 02 and 08

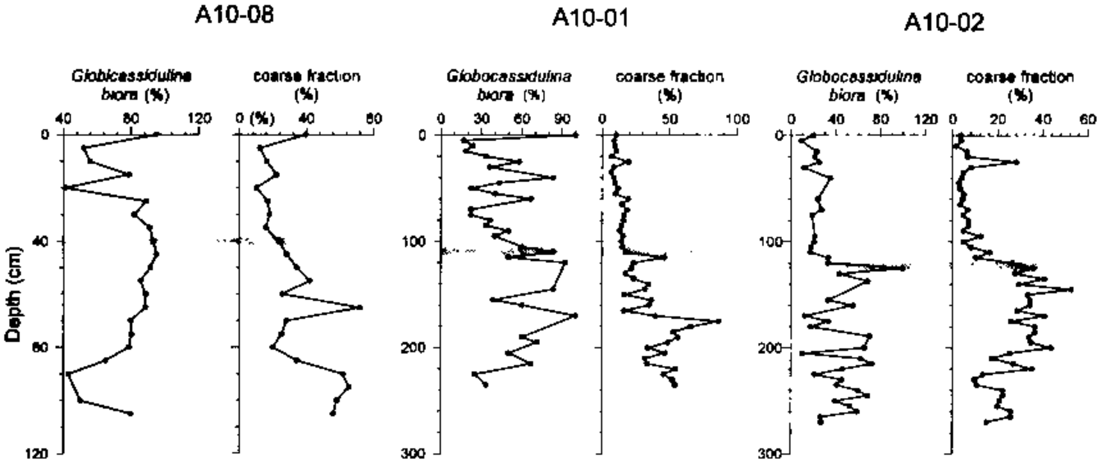

Figure 2-7 Comparison of *Globocassidulina biora* relative abundance with coarse fractions (%, >0.063mm)

species, but core A10-08 constitutes none of this arenaceous species. This may reflect the different water masses in different water depth. Core A10-02 is influenced by erosive water, even though it is just 50 m deeper than core A10-08

The foraminifera absolute abundances have a higher value in the upper parts of three cores(even though considering the differences of sedimentary rates in these two parts). The higher foraminiferal abundances can be correlated to the higher contents of total organic carbon (TOC, Fig. 2-9). The higher flux of organic material into the sediments is regard as a contribution to the higher productivity of benthic foraminifera.

The abundances of these species have a frequent large-range vibration either in the relative higher or lower percentage periods. We think it reflects the characteristic of the Antarctic environment, more fluctuations than in the lower latitude areas. However, because there is only a few age controls, it is difficult to monitor the short time climatic changes and to analyze their cycles.

2-4-3. Foraminiferal dissolution and paleoceanographic changes

2-4-3-1 Down-core variation of Benthic foraminiferal dissolution index (BDI)

The specimens of core A10-08 are mostly polished, very shine in appearance (higher value BDI, most higher than 0); while in core A10-02, the benthic foraminifera is composed of shells with vague, rough surface (lower value of BDI, less than 0) (Fig. 2-8). The fragmentation also reflects the foraminiferal dissolution: In core A10-08, there are few broken specimens (lower fragmentation, less than 25 percent) while core A10-02 has much more broken shells(higher fragmentation, sometimes 100 percent).

The down core variations of benthic foraminifera dissolution index show the same trend. There is a higher value in the lower parts of three cores, compared with those of their

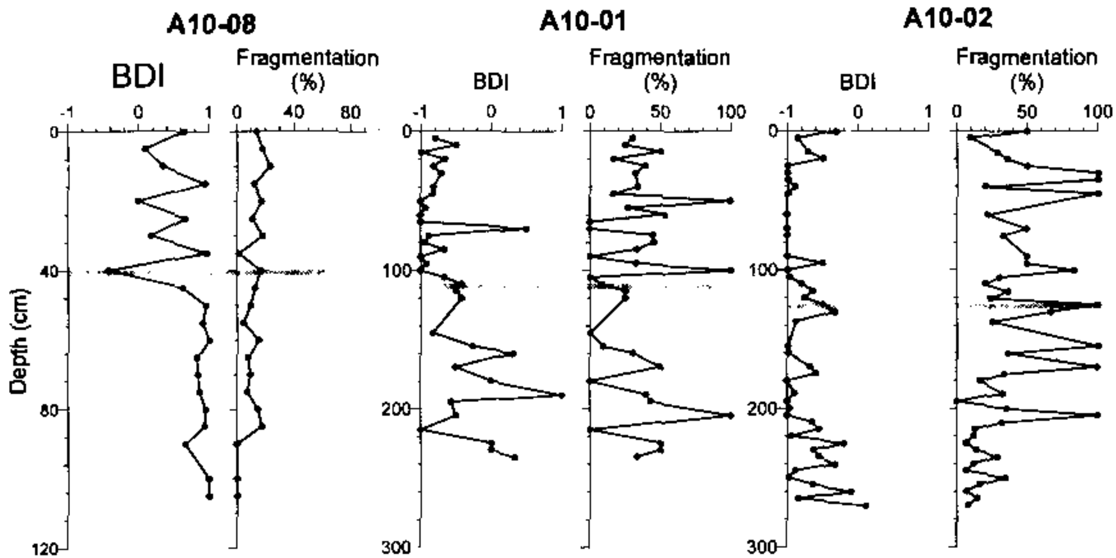

Figure 2-8. Down-core $CaCO_3$ dissolution index (BDI and fragmentation)
in cores A10-01, 02 and 08

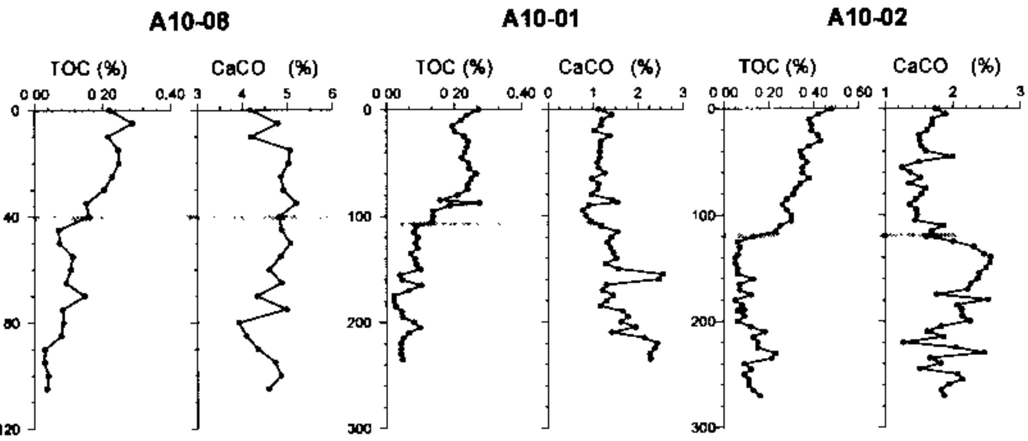

Figure 2-9 Down-core variations of total organic carbon (TOC) and $CaCO_3$ in cores A10-01, 02 and 08

upper parts. This reflects the carbonate dissolution was week in the lower parts and stronger in the upper parts of the cores. The difference of dissolution can be observed from the shell surface microstructure of benthic foraminifera *Globocassidulina biora*. As shown in Fig. 2-3, the polished , shine shells have a smooth surface with very finely perforate micro-crystal in the lower part of core A10-01 (depths 115 cm and 135 cm) while the shells of vague appearance have a rough surface with erosive remnants of microcrystal in the upper part of core A10-01 (depths 15 cm and 75 cm).

2-4-3-2 Variations of $CaCO_3$ and TOC contents, C/N ratio and the factors controlling the carbonate dissolution

The carbonate contents also reflect the variation of the dissolution in three cores. In Fig. 2-9, $CaCO_3$ show a higher percentage (about 1.7% and 2% in average) in the lower parts compared with those (average 1% and 1.5%) of the upper parts of core A10-01 and 02, respectively. The higher $CaCO_3$ contents in the lower part indicate a week dissolution of the sediment carbonate in three cores at the earlier sedimentation period (last glaciation).

As shown in Fig. 2-9, the lower $CaCO_3$ content can be correlated with a higher content of Total organic carbon (TOC) in these cores. We consider the higher TOC content is one of the reasons which led to the stronger dissolution in their upper parts. Higher content of organic material in the sediment increased the accumulating of more CO_2 content in sedimentary water by the bacterial degeneration and then enhanced the dissolution of carbonate (both terrestrial and marine sources) in the upper parts of the study cores. This suggestion was also supported by the results of total sulfur content (Kim *et al.*, 1998), which implies a relatively higher input of organic matter of marine origin.

Though the stronger dissolution happened in the upper parts of three cores, we can see that benthic foraminifera still have a higher abundance in the sediment. Hence, the variation of the abundance mainly reflects the production connected with the food source. This can be explained by the dissolution mechanism of calcareous foraminifera. In modern oceans, the living foraminifera is protected by the protoplasm from dissolution. The dissolution of foraminifera mostly happen in the sediment after their death. Therefore, we can still observe the stronger influence of $CaCO_3$ dissolution from the surface structure of the foraminiferal shell in these sediments.

When comparing the $CaCO_3$ of Core A10-01, 02 with that of core A10-08, we found that core A10-08 was less affected by the dissolution, with a generally high content of carbonate(average 4.5%, twice more than those of core A10-01 and 02) and well-preserved foraminifera shells (lower BDI).

The difference among the dissolution of three cores reflected that the main factor controlling the $CaCO_3$ is not the TOC but water masses in different water depths. In Antarctic area the CCD is much shallow compared with that of lower latitude. Kennett (1966) reported a shallow CCD of 500 m in the Ross Sea due to the high concentration of carbon dioxide. In the Weddell Sea, the CCD may vary from 3000 to 250 m, because of the influence of water mass---- the erosive Saline Shelf Water (Anderson, 1975). From our observation from the sediment of the Maxwell Bay, the CCD is also much shallower (it may be even around 100 m) because in sediments with water depth more than about 100 m, the foraminifera fauna mostly composed of agglutinated species (unpublished personal material).

2-4-3-3 Paleoceanographic changes since the last deglaciation

Benthic foraminifera and geochemical analyses of cores A10-08,01 and 02 from the Maxwell Bay provide the evidence of paleoceanographic changes since the last deglaciation.

<u>The last deglaciation</u> (about 15,400-10,000 cal. yr BP) The water was covered by the sea- ice with a very low primary productivity based on the lower TOC in sediment. The less

flux of marine organic material resulted in the lower benthic foraminiferal productivity (lower abundance). However, the foraminiferal shell characteristics (BDI, and Fragmentation) indicated a well-preservation of carbonate during this time. It is supposed that the water was less erosive due to the weak influence of Saline Shelf Water at the lower sea level.

Post glacial (about 10,000-5,500 cal. yr BP) with the retreat of groundlime of coastal glacier and less coverage of sea ice in the Maxwell Bay, the surface primary productivity increased rapidly. This caused the high input of marine organic material into the sediment (higher TOC and lower C/N ratio in the upper parts of study cores). The water became more erosive due to the stronger influences of Saline Shelf Water and enhanced by the accumulation of CO_2 in the sediment (degenerated from higher TOC by the bacteria). Therefore, the $CaCO_3$ in the sediment is much lower than that of the last deglaciation and the benthic foraminifera also showed a stronger dissolution at this time.

2-5. Discussion

2-5-1. Ecology and distribution of Globocassidulina biora and its relationship with paleoenvironmental changes in Antarctica

Calcareous benthic foraminifera *Globocassidulina* spp. (including *G. subglobosa*, *G. crassa*, *G. crassarossensis* and *G. biora*) dominate the shallow shelf water (Milam and Anderson, 1981), mostly in the coarse-grained sediments. In the Great Wall Cove of Maxwell Bay, only one species of *G. biora* was found on the modern coarse muddy-sand by Chen & Zhan (1991). Though many species of benthic foraminifera had been recognized and they displayed a high diversity in the surface sediments of Marian Cove (Chang & Yoon, 1995), much less species were reported from core samples of late Holocene at the same area and *G.*

biora ranged from 55% to 98% with the average value of 90% of total fauna (Park *et al.*, 1995; Woo *et al.*, 1996). Therefore, it is the most important species in understanding the paleoclimatic and paleoceanographic changes of the Antarctic shallow water

G biora, first described from recent Westfold Hill by Crespin (1960), is a infauna-type and free-moving benthic foraminifera, lived most in the antarctic shallow water with temperature range from -1.95 to -1.14□□C and salinity from 33.96 to 34.99 ‰. It favors an anoxia sediments with with low diversity (H(s) = 0.667-1.10) while other types of benthic foraminifera rarely survive (Bernhard, 1987; Murray, 1991).

It was supposed that benthic foraminifera *G. biora* has kept a strong resistance to the high-energy-mechanical erosion because of its large and thick shell (Li & Li, 1996), which often yields with a high abundance in the thanatocoenoses of coarse sediments than those in the living fauna or in the fine sediments. Therefor, its appearance with high abundance often implies the near-shore shallow high-energy environment.

However, Maybe the important factors controlling the changes of *G. biora* in the studied area are water temperature, salinity, dissolution, or nutrients which connected with the climate change instead of sedimentary substrate. Due to only few work has been carried out on the investigation of its ecology, there is great limit to reconstruct paleoclimate using the change of *G biora* in late Quaternary sediments.

2-5-2. AMS ^{14}C age problem

Park *et al.* (1995) and Yoon *et al.*(1998) suggested deglaciation around 4700 cal. yr BP in the core S-19 of the same area (Fig. 2-1), but our result proposed that the deglaciation should happen around 10,000 cal. yr BP. Kim (1998) suggested a ^{14}C reservoir correcrion of 5200 years in core A10-01, and 1200 years in core S-19. If so, the climate history of these study cores can be correlated with that of Core S-2 of Admiral Bay and Core S-19 of Maxwell

Bay in the King George Island. Domack *et al.* (1989) also reported an old age of surface sediment of East Antarctic continental Shelf. It might be possible to have a ^{14}C reservoir of ~5000 years Another possibility is that we lost some surface sample because of the technology of piston core. However, this needs more work on the box cores and more ^{14}C dates to solve the chronology difference of in such a near core (S-19 and A 10-01).

2-6. Conclusions

The foraminifera assemblages from the Maxwell Bay are controlled by the plaeo-environment. During the last glaciation, benthic forammifera had a lower abundance due to the low productivity, but they were well-preserved, consistent with the high content of $CaCO_3$ in the sediments. The *Globocassidulina biora* showed some connection with the coarse sediment (ice-proxomal diamiction or rhythmite), have a higher abundance in this deglaciation. After glacial, with the deepening and less ice-coverage of water, high surface productivity increased the benthic foraminiferal abundance by providing more organic particles. At the same time, the high organic carbon accumulated in the sediments enhanced the dissolution of $CaCO_3$ deposit.

The difference of benthic foraminiferal assemblage and $CaCO_3$ between core A10-08 and A10-02 implies two different water masses controlling these cores, even though the water depth of core A10-02 is only 50 m deeper than that of Core A10-08. There exist lower $CaCO_3$, lower BDI, high fragmentation and higher percentage of arenaceous *Miliammina arenacea* in core A10-02, it might be affected by the erosive Saline Shelf Water even in the depth of 100 m.

Therefore, we think the most important factors affecting the sediment in shallow glacial marine environment of Maxwell Bay are the water masses (such as Saline Shelf Water) and their controlling very shallow CCD, besides the advance or retreat of coastal glacier with sea-level changes during the late Quaternary glacial cycles.

제 3 장 남극 드랜스필드 해협 퇴적물에서 탄소, 규소, 안에 대한 지화학적 연구

Chapter 3 Geochemistry of carbon, silica, sulfur, and phosphorus in the Bransfield Strait sediments, Antarctica.

3-1. Abstract

Downcore profiles of biogenic silica (Bsi), total organic carbon (TOC), total sulfur (TS), calcium carbonate, and inoganic phosphorus (IP) contetns were determined to investigate the major factors controlling their downcore variations in the Bransfield Strait sediments. These biogenic elements show large downcore variations. The downcore variations of Bsi and TOC contents are mostly derived by biogenic production changes in the water column. Especially, the cyclical downcore variation of Bsi contents reflects that marine productiviry has periodically changes over times in Brasfild Strait. TS contents show a similar downcore variation with TOC contents, implying that sulfide minerals are enriched in organic-rich sediments. Calcium carbonate contents display quite different dowcore profiles with Bsi and TOC contents. IP contents show a contrary trend in their downcore distribution with Bsi and TOC contents, suggesting that IP is mostly composed of detrital phosphorus minerals and that authigenic phosphorus minerals do not form in the Bransfield Strait sediments.

3-2. Introduction

Bransfield Strait is a basin that lies between the South Shetland Islands and the tip of the Antarctic Peninsula (Fig. 1). It is approximately 100 km wide by 400 km long and is bounded on the northwest by steep normal faults. The axial depth of the basin varies from 1100 m in the southwest to 2800 m in the northeast, south of Elephant Island (Baker and Griffith, 1972). Bransfield Strait is an active marginal basin in a back-arc tectonic setting (Baker and Dalziel, 1983). Submarine volcanism and hydrothermal activity has been observed (Whiticar et al., 1985). Duriug the austral winter sea ice covers entirely Brasfield Strait resulting in minimal primary productivity, meanwhile, the sea surface is completely sea ice-free in the summer, giving rise to increased productivity (Wefer et al., 1990).

There are many researches to elucidate sedimentary processes in Bransfield Strait (Anderson and Molnia, 1989; Jeffers and Anderson, 1990; Yoon et al., 1992; Yoon, 1996). Biosiliceous ooze, terrigenous muds, and ice-rafted gravels are dominant components in the bottom sediments of Bransfield Strait (Yoon et al, 1992). Volcanic ash from submarine and subaerial eruptions are also considerably contained in the bottom sediments (Anderson and Molnia, 1989). However, geochemical studies have been rarely conducted (Keller et al., 1991). The main objective of this study is to describe downcore variations of biogenic elements, such as biogenic silica, organic carbon, total sulfur, and inorganic phosphorus and to determine major factors controlling their downcore variations. We also try to elucidate paleoenvironmental changes in Bransfield Strait based on the downcore variations of biogenic elements.

3-3. Material and Methods

Two sediment cores were collected with a gravity corer from Bransfield Strait during the fifth Korea Antarctic research programs conducted by Korea Ocean Research and Development Institute Core S15 was obtained at a water depth of 1220 m in the southwest Bransfield Strait, and core EB2 was at a water depth of 2200 m in the northeast Bransfield Strait (Fig. 3-1). Subsamples was taken at 10 cm intervals. Sediment grain size was analyzed by a Micometrics Sedigraph 5000D for silt and clay fractions (4 to 10 ϕ) and by dry sieving for sand fraction (-4 to 4 ϕ). Each sample was dried at 80 ℃ for 4 days and then grounded to determine biogenic silica, total organic carbon, total sulfur, and inorganic phosphorus contents. Biogenic silica contents were determined by leaching with 40 ml of a 2M Na_2CO_3 solution for 5 hours at 85 ℃ (Mortlock and Froelich, 1989). Total organic carbon contents were determined by a Carlo-Erba CNS analyzer after eliminating inorganic carbon by 10 % HCl. Total sulfur contents were also measured by the same CNS analyzer. Calcium carbonate contents were determined by subtracting total organic carbon contents from total carbon contents which were measured without any treatment by the CNS analyzer. Inorganic phosphorus contents were determined after continuous shaking for 16 hours in 1.0 N HCl at a room temperature (Aspila et al., 1976).

3-4. Results and Discussion

3-4-1. Biogenic silica

At core S15 biogenic silica (Bsi) shows a large downcore variation, ranging from 10 to 20 wt. % (Fig. 3-2a). High Bsi contents are observed at the sediment depths of 90, 130, 180, 290, 370, 470 cm, displaying somewhat a cyclical change with sediment depth. At core EB2

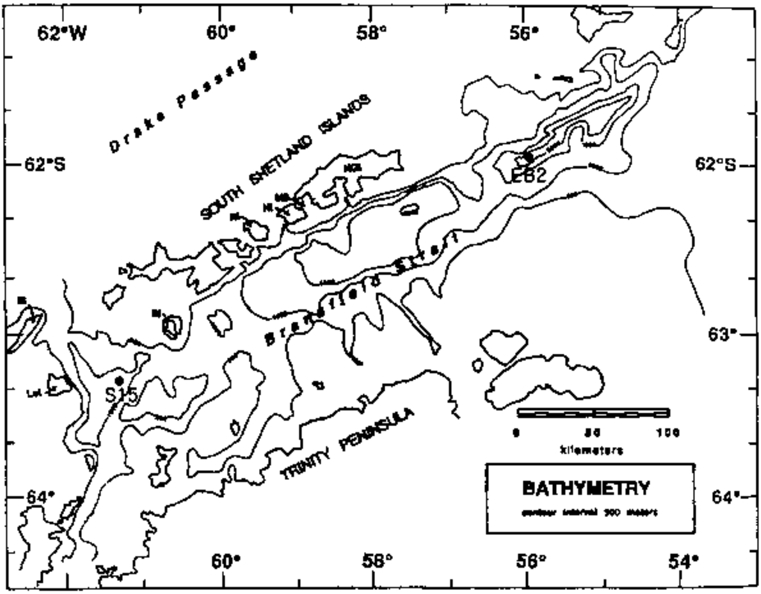

Figure 3-1. Geography and bathymetry of Bransfield Strait. Black circles indicate sediment core sites. KGI = King George Island, MB = Maxwell Bay, NI = Nelson Island, RI = Robert Island, DI = Deception Island, SI = Smith Island, and LoI = Low Island

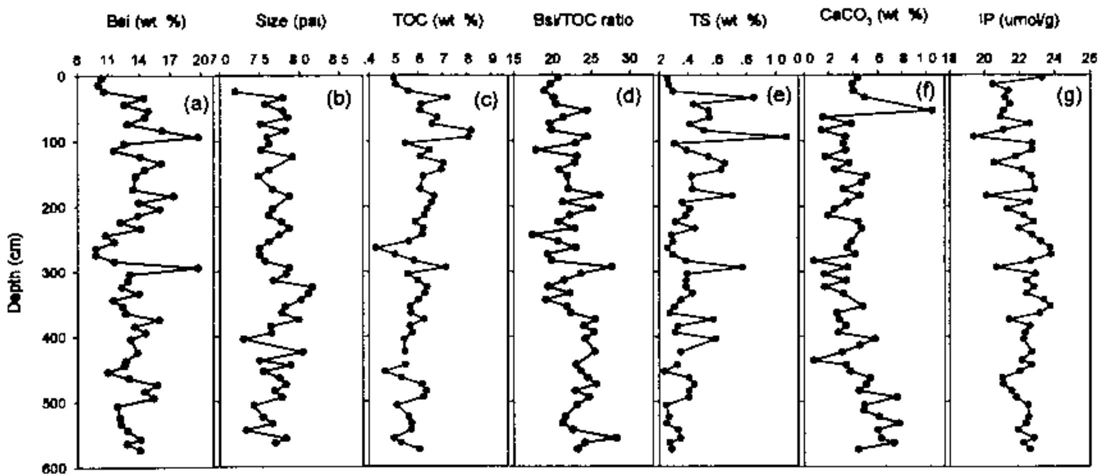

Figure 3-2. Downcore profiles of (a) Bsi, (b) sediment grain size, (c) TOC, (d) Bsi/TOC ratio, (e) TS, (f) calcium carbonate, and (g) IP at core S15 of Bransfield Strait

Bsi contents vary from 16 to 40 wt. % and are almost twice as high as those at core S15 (Fig. 3-3a). Bsi contents are relatively low in the upper 110 cm and consistently greater than 20 wt. % below 110 cm. Basically, Bsi contents in marine sediments depend on three factors; biogenic production in the water column, dissolution in the sediments, and dilution with terrestrial materials (Leinen et al., 1986; Rea et al., 1991; Archer et al., 1992). If the dissolution is a major factor controlling Bsi contents in the sediments, Bsi contentes would decrease vertically because more dissolution occurs at the deeper sediments. At both cores Bsi contents fairly oscillate with sediment depth, not showing clearly a downcore decrease trend (Figs. 3-2a and 3-3a), which implies that Bsi contents are not significantly influenced by the dissolution in the sediments. Therefore, the downcore variations of Bsi contents are derived either by biogenic production changes or by input flux changes of terrestrial materials.

Strong surface currents (50 - 100 cm/s) have been observed in Bransfield Strait (Huntley et al., 1991). Because the two core sites are located below 1000 m water depth, bottom sediments are not directly influenced by such strong currents. However, the suspended sediments induced by strong currents in continental shelves or upper slopes can be transported along steep slopes of Bransfield Strait and deposited in the deeper basins. Therefore, many turbidites and contourites have been often found in several sediment cores obtained in Bransfield Strait (Yoon, 1995). Several samll-scale (2-5 cm) contourite deposits are also observed at core S15 (Yoon, 1995). Because sediment samples are collected at the depth intervals where contourite deposits are not found, however, Bsi contents at core S15 are not considerably influenced by contourite deposits. At core S15 sediment grain size show a small variation with sediment depth, ranging from 7.2 to 8.2 ϕ (Fig. 3-2b). Downcore variation of sediment grain size does not show any correlation with that of Bsi contents (Figs. 3-2a and 3-2b). Consequently, the downcore variations of Bsi contents are most likely caused by biogenic production changes in the water column. At core EB2 sediment grain size varies from 9.0 to

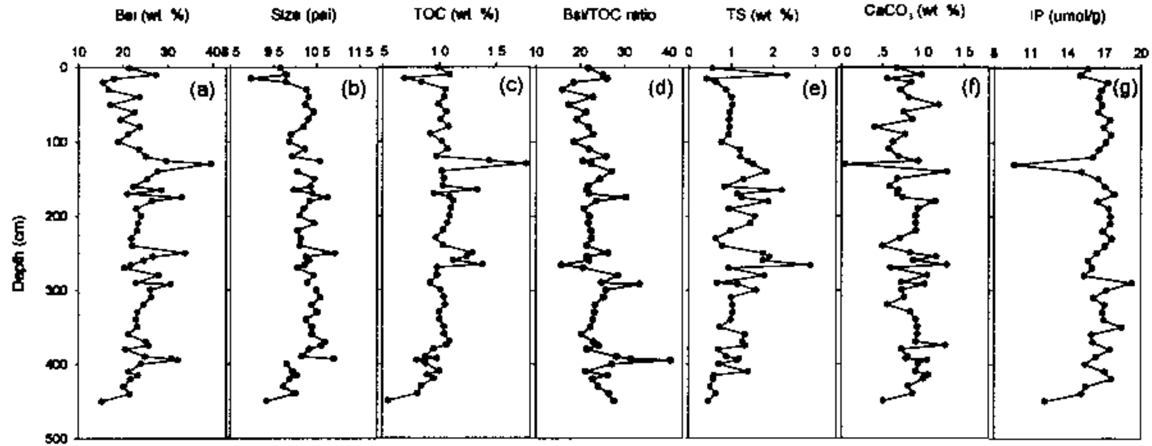

Figure 3-3. Downcore profiles of (a) Bsi, (b) sediment grain size, (c) TOC, (d) Bsi/TOC ratio, (e) TS, (f) calcium carbonate, and (g) IP at core EB2 of Bransfield Strait

10.9 ϕ and is finer than at core S15 (Fig. 3-3b). Downcore variation of sediment grain size also does not show any relatioship with that of Bsi contents (Figs. 3-3a and 3-3b). At core EB2 turbidite deposits are found at a depth interval of 20 - 90 cm and well laminated sediments are dominant below 90 cm (KORDI, 1996). Bsi contents are relatively low at the turbidite deposits and high at the laminated sediments. Therefore, Bsi contents at the 20 – 90 cm depth interval are affected by terrigenous sedimentation, and the downcore variation below 90 cm is mostly derived by the biogenic production changes in the water column.

3-4-2. Total organic carbon

At core S15 total organic carbon (TOC) contents range from 0.43 to 0.82 wt. % and display a large downcore variation (Fig. 3-2c). At core EB2 TOC contents fluctuate around an average value of 1.0 wt. % with a maximum value of 1.8 wt. % at 130 cm and a minimum of 0.6 wt. % at the bottom of the core (Fig. 3-3c). In general, TOC content of the modern sediments is controlled by biogenic production in the water column, preservation in the sediments, and dilution by terrigenous sedimentation and reworking of bottom sediments (Calvert, 1987; Berger et al., 1989; Domack et al., 1993). In the previous section, it is suggested that at both cores the downcore variations of Bsi contents are mostly caused by biogenic production changes in the water column, except at the 20 – 90 cm depth interval. TOC contents show a similar downcore distribution pattern with Bsi contents(Figs. 3-2c and 3-3c), reflecting that TOC contents are also controlled mainly by biogenic production in the water column

At core S15 Bsi/TOC weight ratio varies from 17.4 to 28.2, with an average of 22.4 (Fig. 3-2d), and high Bsi/TOC ratios generally correspond to high Bsi and TOC contents. At core EB2 Bsi/TOC ratio ranges from 15.7 to 40.3, with an average of 23.5 (Fig. 3-3d), which is similar to that of core S15. These Bsi/TOC ratios are about 30 times higher than that of living marine diatom (0.81) (Brzezinski, 1985). Leynaert et al. (1993) found that Bsi/TOC weight ratios in particulate matter collected in water column of the Weddell Sea varied from 0.10 to 0.30, with an average of 0.20. The extremely high Bsi/TOC ratios at these two cores implies that decomposition of organic matter is much more significant in the water columns and sediments than Bsi dissolution in Brasfield Strait. The Bsi/TOC ratios in the Brasfield Strait sediments are higher than those (an average of 14.2) in the Maxwell Bay sediments (Kim et al., 1998), reflecting that decomposition of organic matter is more intensively occurring in Bransfield Strait than in Maxwell Bay due to a deep water depth and a relatively low sedimentation rate.

3-4-3. Total sulfur

At core S15 total sulfur (TS) also exhibits a similar downcore variation with TOC with a range of 0.25 - 1.07 wt. % (Fig. 3-2e). At core EB2 TS contents vary from 0.4 to 2.9 wt. % and are somewhat higher than at core S15 (Fig. 3-3e). The downcore pattern in TS contents also parallels that of TOC contents. TS is mostly composed of reduced sulfur, such as pyrite which forms due to the reaction of hydrogen sulfide with reactive iron (Berner, 1984). Bacteria-mediated sulfate reduction occurs intensively in organic-rich marine sediments. As a result, hydrogen sulfide, a by-product of sulfate reduction, forms and reacts with reactive iron to form pyrite. Thus pyrite is enriched in organic-rich sediments, which helps to explain the well correlation between TOC and TS.

The carbon-sulfur relationship has been actively used to interpret paleoenvironments of both modern and ancient sedimentary sequences (Raiswell and Berner, 1985; Dean and Arthur, 1989; Morse and Emeis, 1990; Rao et al., 1994). In normal marine sediments the organic carbon to reduced sulfur (C/S) ratio averages 2.8 ± 0.8 (Berner, 1982). In the sediments of freshwater or brackish environments, the C/S ratio is much higher than in normal marine sediments because of much less diagenetic pyrite formation in the sediments laid down in freshwater which contains less dissolved sulfate compared to seawater (Berner and Raiswell, 1984). In anoxic environments such as the Black Sea, however, the C/S ratio is lower than the normal C/S ratio because pyrite can form in the water column, and sulfide can be supplied to these sediments from overlying waters (Leventhal, 1983; Raiswell and Berner, 1985).

At core S15 TOC/TS weight ratios range from 0.75 to 2.29 with an average of 1.58, meanwhile at core EB2 they vary from 0.47 to 1.75 with an average of 1.01 (Fig. 3-4). At both cores TOC/TS ratios are lower than the C/S weight ratio (2.8 ± 0.8) in normal marine sediments These low C/S ratios are usually observed in anoxic environments where hydrogen sulfide is present in bottom waters (Leventhal, 1983; Rao et al., 1996). In Bransfield Strait, strong surface currents are observed, and bottom waters below a 500 m water depth are highly oxygenated (Gordon and Nowlin, 1978). Thus, it is unlike that Bransfied Strait has experienced an anoxic bottom water condition. Consequently, the low C/S ratios observed in the Bransfield Strait sediments do not seem to be derived by an anoxic bottom water condition. There may be two possibilities to explain the low C/S ratio. The first possibility is that a considerable amount of organic sulfur may be contained in TS. In normal marine sediments, organic sulfur usually makes up only a few percent of the TS content (Berner and Westrich, 1985; Francoise, 1987). In the sediments with high sulfate reduction rates, however, various unsaturated lipid react with sulfide to yield sulfur-bearing organic compound (Mossmann et al., 1991; Wakeham et al., 1995) In salt marsh and estuarine sediments, 40 – 60 % of the sulfur can be present in the organic fraction (Ferdelman et al., 1991; Bruchert and Pratt, 1996). In order to elucidate this possibility, we need more works, such as sulfur speciation. The other one is that detrital pyrite is included in TS. It was suggested that the hyderthermal-orgin pyrite has been delivered in Maxwell Bay from King George Island (Kim et al., 1998). Thus, detrital pyrite can be transported into the Bransfield Strait. However, the extremely low C/S ratios (less than 1.0)

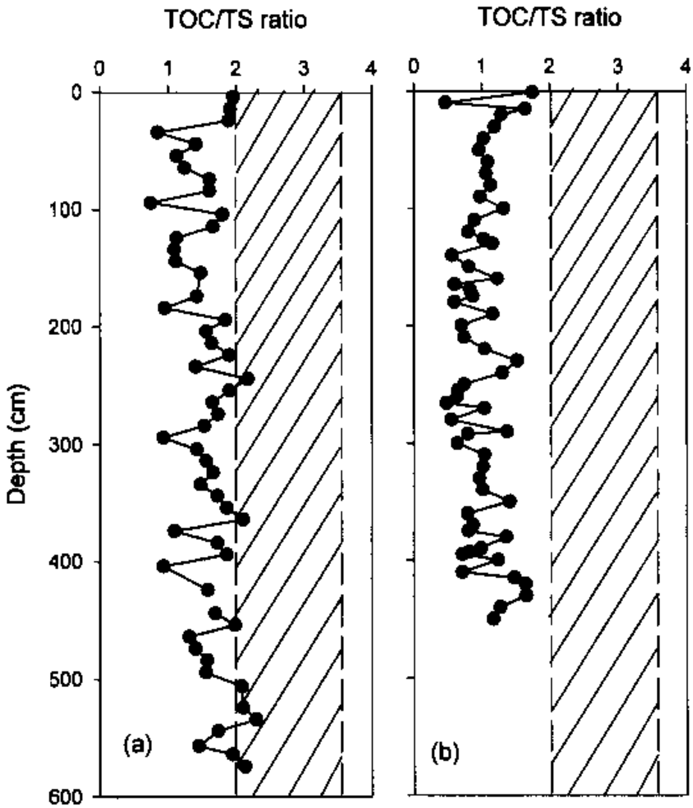

Figure 3-4. Downcore variations of TOC/TS ratio at core S15 and (b) core EB2. Hatched area indicates the range of TOC/TS ratios in normal marine sediments (Berner, 1982)

correspond to the high Bsi and TOC contents at both cores (Figs 3-2, 3-3 and 3-4). Terrigenous material is usually scarce in the sediments of high biogenic contents and thereby, detrital pyrite is relatively poor in these sediments. Therefore, this possibility is less significant compared to the first one.

3-4-4. Calcium carbonate

Calcium carbonate contents vary from 0.1 to 1.1 wt. % with an average of 0.4 wt. % at core S15 and are relatively high at the upper and lower part of the core (Fig. 3-2f). At core EB2 they fluctuate around an average value of 0.82 wt. % and are somewhat higher than at core EB2 (Fig. 3-3f). These calcium carbonate contents are significantly low compared to those at other deep-sea sediments (Karlin et al., 1992; Howard and Prell, 1994). In Bransfield Strait, foraminifera are rarely found at the deeper than 1000 m water depth due to the shallow carbonate compensation depth (CCD) (Yoon, 1995). The water temperature of Bransfield Strait is usually lower than 2 ℃ even in austral summer (Niler et al., 1991), of which cold water causes the CCD to be shallower than 1000 m water depth. Thus, the shallow CCD causes the calcium carbonate content to be extremely low at both cores where water depth is deeper than 1000 m. At both cores the downcore trend of calcium carbonate is not correlated with those of Bsi and TOC (Figs. 3-2 and 3-3), indicating that the downcore variations of calcium carbonate is not derived by the biogenic production changes in the water column.

3-4-5. Inorganic phosphorus

At core S15 inorganic phosphorus (IP) shows a large downcore variation, ranging from 19.4 to 23.8 μmol/g (Fig. 3-2g). At core EB2 IP contents fluctuate around an average of 16.4 μmol/g with a large decrease at 120 cm sediment depth (Fig. 3-3g). At both cores IP contents shows a quite different downcore variation from those of Bsi and TOC contents (Figs. 3-2 and

3-3). Phosphorus has been used for as a proxy for paleoproductivity on a geologic time scale because phosphorus acts as a limiting nutrient for marine productivity (Compton et al., 1993; Kump, 1993; Filippelli and Delaney, 1994; Van Cappellen and Ingall, 1994). Organic phosphorus is transformed to IP by diagenetic processes in marine sediments (Ruttenberg and Berner, 1993, Kim, 1996). In organic-rich sediments, organic phosphorus is remineralized by bacteria metabolism, and dissolved phosphate, a by-product of organic phosphorus remineralization, is produced and accumulated in pore water. As the dissolved phosphate concentration in pore water becomes high, authigenic phosphorus minerals such as carbonate fluorapatite can be precipitated directly form pore water and accumulated in the sediments. Therefore, IP is enriched in organic-rich sediments.

At both cores, however, IP contents are negatively correlated with TOC contents (Fig. 3-5), which indicates that authigenic phosphorus minerals do not form by the diagenetic process in these sediments. The authigenic phosphorus minerals do not form in organic-poor sediments because the dissolved phosphate concentration produced by organic phosphorus remineralization cannot be high enough to precipitate the phosphorus minerals in these sediments. In the Bransfiled Strait, phosphorus cannot be used as a proxy for paleoproductivity because authigenic phosphorus minerals do not form in these sediments. The negative correlation between IP and TOC contents also implies that IP is mostly composed of detrital phosphorus minerals because TOC contents usually decrease as input fluxes of detrital material increase in marine sediments. IP contents are about 5 μmol/g higher at core S15 than at core EB2, and sediment grain size is coarser at core S15 (Figs. 3-2 and 3-3), which indicates that input of terrestrial materials is larger at core S15 than at core EB2.

3-4-6. Implications for paleoproductivity changes

At the surface sediments of core S19 Bsi and TOC contents are 10.4 and 0.50 wt. %,

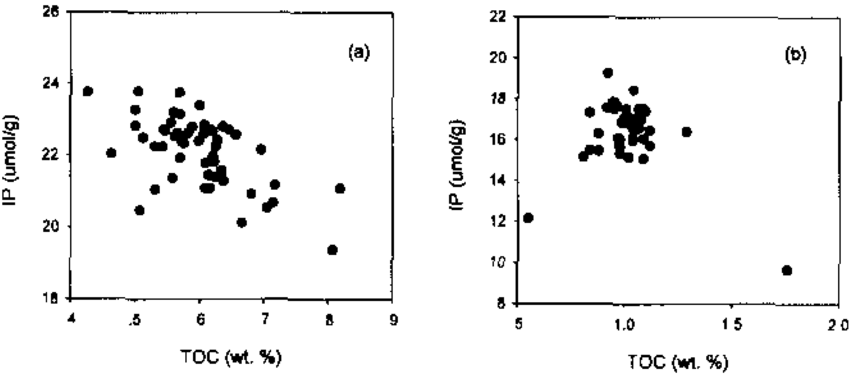

Figure 3-5 TOC contents vs. IP contents at (a) core S15 and (b) core EB2

respectively (Fig. 3-2), which are almost two time lower than those (21.3 and 0.98 wt. %) at the surface sediments of core EB2 (Fig. 3-3). Based on the higher IP content and coarser sediment grain size at core S19, it was suggested that input of terrestrial materials is larger at the core S15 site than at the core EB2 site. Primary production at the core S15 site is 650 mg C m^{-2} d^{-1} (KORDI, 1995), but is not available at the core EB2 site. Considering that primary production is generally higher in the southeastern Bransfield Strait than in the northwestern Bransfield Strait (KORDI, 1995), however, it may be higher at the core EB2 site. Thus, the higher Bsi and TOC contents at core EB2 site are ascribed to the less input of terrestrial materials and higher primary production.

In the previous section, it was suggested that at cores S15 and EB2 the downcore variation of Bsi contents is mostly derived by the biogenic production change in the water column, except at the 20 – 90 cm depth interval of core EB2. At core S15 Bsi contents show a cyclical downcore variation, implying that marine productivity has periodically changed over times At core EB2 Bsi contents also show a somewhat cyclical downcore variation below 90 cm. The cyclical change in marine productivity may be derived by the climatic change: high productivity occurred at warm period, and low productivity at cold period. In Antarctic Ocean, warm climate causes the annual coverage of sea ice to be reduced (Jacobs and Comiso, 1993) Thus, marine productivity may increase at the warm climatic condition. The cyclical changes in marine productivity are also observed in other Antarctic areas: Leventer et al. (1996) suggested that marine productivity has cyclically changed by a period of 200 – 300 years in the Antarctic Peninsula region. They also suggested that the cyclical productivity changes are caused by climatic changes mediated by solar radiation modulation. Domack et al. (1993) found 300-year cyclicity in organic matter preservation resulted from either temporal variations of marine productivity or changes in the terrigenous sediment supply in the Antarctic fjord sediments.

3-5. Summary

At the two sediment cores obtained from Bransfield Strait, the contents of biogenic elements show large downcore variations. Bsi contents do not seem to be significantly influenced by its dissolution in the sediments and terrigenous sedimentation. The downcore variation of Bsi contents is mostly derived by biogenic production changes in the water column. TOC contents exhibit a similar downcore variation with Bsi contents, suggesting that they are also controlled mainly by biogenic production in the water column. Bsi/TOC weight ratios vary from 17.4 to 28.2 at core S15 and from 15.7 to 40.3 at core EB2, of which ratios are higher than those in the Maxwell Bay sediments, reflecting that decomposition of organic matter is more actively occurring in Bransfield Strait. TS contents show a similar downcore variation with TOC contents, implying that sulfide minerals are enriched in organic-rich sediments. TOC/TS weight ratios range from 0.75 to 2.29 with an average of 1.58 at core S15 and from 0.47 to 1.75 with an average of 1.01 at core EB2, of which ratios are much lower than those in normal marine sediments. The reason for the lower TOC/TS ratio in the Brasfield Strait sediments can not be clearly explained, and thereby, we need more works, such as sulfur speciation. Calcium carbonate contents are extremely low (0.1 to 1.3 wt. %) compared to those in other deep sea sediments, which is due to shallow CCD caused by the very cold seawater temperature. IP contents are negatively correlated with TOC contents, indicating that IP is mostly composed of detrital phosphorus minerals and that authigenic phosphorus minerals do not form in the Bransfield Strait sediments.

제 4 장 동지나해 북 대륙붕에서 빙하기 이후 고해양학적 기록에 대한 연구

Chapter 4 Paleoceanographic Records from the Northern Shelf of the East China Sea after the Last Glacial Maximum

4-1. Abstract

Both benthic and planktonic foraminifera from core 97-02 obtained in the northern East China Sea are quantitatively analyzed for reconstructing the paleocenography of late Quaternary. Since the earliest time of the core sediment (not older than 18,000 yr B.P.), the paleo-water depth has changed from less than 20 m to near 100 m at present, which are reflected by the benthic foraminiferal assemblages: before 14,000 yr B.P., the water depth was shallower than 20 m; from 14,000 to 7,500 yr B.P., 20-50 m in water depth; and after 7,500 yr B.P., 50-100 m in water depth. The foraminiferal fauna also disclose the water mass history: during the last glacial, the water dominated the study area might be the coastal water; at the end of the last glacial (14,000-10,000 yr B.P.), the Yellow Sea cold water mostly affected this area; then it gave way to the Yellow Sea Warm Current after 10,000 yr B.P.; and finally the warm water dominated this area after 7,500 yr B.P., due to the westward shift and enhancement of the Kuroshio Current.

4-2. Introduction

The last glacial cycle has been more concerned in the study of the East China Sea paleoceanography (Wang, 1990, Yan & Thompson, 1991; Ujiie *et al.*, 1991). Through the interpretation of paleo-climate, we can understand much more about the mechanism of climatic change and have a better knowledge of what it will be in future. Most works have been done on the paleoceanographic and paleoclimatic reconstruction through the continuous semi-deep sea sediment in this area (Wang, 1992; Xu and Oda, 1994; Jian *et al.*, 1996; Li *et al*, 1997). For the reason of poor-preservation of the sediments during the glacial cycles, the land-ocean interaction belt or the shallow-water shelf sediment were often ignored. In fact, however, it provides a direct record of the climatic changes on the near land, and at the same time, the paleoceanographic changes in these shelves may affect the coastal life very much. For example, the rising of the sea level will change a lot of land areas into sea, and many cities will disappear (Min & Wang, 1979; Yang, 1986).

With the sea level changes, the Kuroshio Current had been shifted to the outside of Ryukyu Islands during the last glacial (Chinzei *et al.*, 1987) and finally returned to the Okinawa Trough about 7,000 years ago (Jian *et al.*, 1998) The shelf of East China Sea has such a big change from being exposed all above the water (Wang, 1992) in the last glacial maximum to the present status. Xu and Oda (1994) reported that there was a notable salinity decrease in the northern slope of East China Sea between 16,000 and 10,000 years ago due to the huge amount discharge of fresh water from the paleo-Yellow River. In that case, there should exist more evidence on the changes of salinity in the shelf area.

Till now, the microfossil analyses of core DZQ-4 from the shelf of East China Sea (Tang, 1996) and of core QC-2 from the Yellow Sea (Yang *et al.*, 1996) are the most detailed work on the shelves. However, since the water depth of core QC-2 is only 49.05 m at present, it has a strong shortcoming in recording the continuous marine strata when the sea level dropped more than 50 m below the present during the late Quaternary as it disclosed from the result of core QC-2; and core DZQ-4 has a stratigraphy of very low resolution for post-glacial case. Thus they can not provide a continuous and detailed information of paleoclimate and paleoceanogaphy.

Recently, we have taken a serial cores from the northern East China Sea. Core 97-02 lies under the Yellow Sea Warm Current (Fig. 4-1). The Coastal Current and Yellow Sea cold water also have an important effect on the sediment of this area (Qin & Zhao, 1986). Though this is only the preliminary results of foraminiferal analysis of core 97-02, it shows itself a good presentation of foraminifera for studying the post-glacial changes of paleo-climate, water depth and water masses.

4-3. Material and methods

Core 97-02 is a 545 cm-long piston core (31°21.67'N, 126°33.11'E) taken at the water depth 93.9 m in October, 1997. It is composed of silty clay (0-60 cm), muddy sand (60-150 cm), silt (150-250 cm) and fine sand (250-545 cm). Thirty-nine samples were collected for the foraminiferal analyses with an interval of 10-20 cm (Table 4-1) and were processed by standard microfossil treatment.

In sediment samples from the study area, the benthic foraminifera were very small-sized and sometimes there were few specimens, so we used the CCl_4 to float the foraminifera, but we still checked the sediment after floating to make sure that all the foraminifera were picked up Benthic foraminifera were analyzed for the larger than 63 μm fractions. The standard for benthic foraminifera identification was based on the description of He *et al.*(1965), Zheng *et al.*

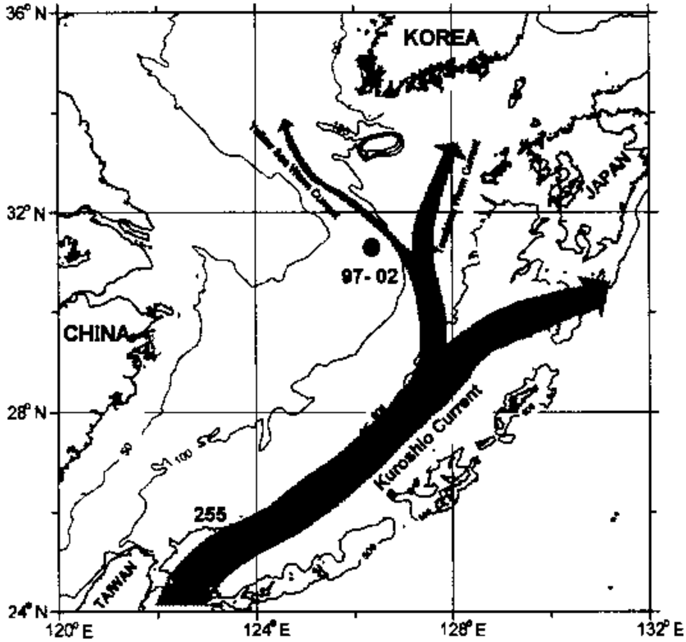

Figure 4-1. Core location and bathymetry of the Easrt China Sea

Table 4-1. Samples of core 97-02 analyzed in this study

depth (cm)	dry weight (gram)	depth (cm)	dry weight (gram)	depth (cm)	dry weight (gram)
0-2	2	130-132	3	260-262	8
10-12	2	140-142	3	270-272	8
20-22	2	150-152	3	280-282	8
30-32	2	160-162	5	300-302	8
40-42	2	170-172	5	320-322	8
50-52	2	180-182	5	340-342	8
60-62	2	190-192	5	360-362	8
70-72	3	200-202	5	380-382	8
80-82	3	210-202	5	400-402	8
90-92	3	220-222	5	420-422	8
100-102	3	230-232	5	460-462	12
110-112	3	240-242	5	480-482	12
120-122	3	250-252	8	510-512	12

(1978) and Wang *et al.* (1988). The benthic foraminifera specimens were mounted on the cardboard slide and counted (Appendix 4-1).

Planktonic foraminifera were identified in the larger than 125 μm fractions (Appendix 4-2) for the comparison with those of other areas. The taxonomy of planktonic foraminifera was followed by Be (1977), Thompson (1981) and Hemleben *et al.* (1988). We also counted the total number of planktonic foraminifera in a greater than 63 μm fractions. Therefore, the planktonic ratio to total foraminifera is calculated based on the numbers of planktonic and benthic foraminifera counted from the large than 63 μm fractions.

We used the Shannon-Wiener information function [H(S)] to calculate the faunal diversity (Gibson and Buzas, 1973). The equation is :

$$H(S) = -\sum_{i=1}^{S} P_i * \ln P_i$$

where S is the number of species or subspecies and P_i is the proportion of the i th species in each sample High value of H(S) indicates great species diversity, and occurs when all species are equally distributed.

4-4. Results

4-4-1. Stratigraphy

Planktonic foraminifera *Pulleniatina obliquiloculata* has shown an important and valid role in subdividing the late Quaternary stratigraphy and reconstructing paleo-ocean environments. The variations of its relative abundance during the glacial/interglacial cycles can be correlated in the northwest Pacific marginal seas (Wang *et al.*, 1996; Li, 1997; Li *et al.*, 1997).

Without the age dating of core 97-02, it is thought a better method to compare this one with core 255 (25°12'N, 123°06'E, water depth 1575 m) from the southern East China Sea. There is a chronological model with a numerous age-control points in core 255 (Li *et al.*, in preparation). From the changes of *Pulleniatina obliquiloculata* between the two cores (Fig. 4-2), we presume the strata at depths of 200 and 270 cm in core 97-02 can be correlated to that of 370 cm (about 10,000 yr B.P.) and roughly at 430 cm (about 12,000 yr B.P) in core 255, respectively. According the average sedimentary rate of 20 cm/ky at the interval of 0 to 200 cm in core 97-02, the strata at depth of 150 cm was interpolated as 7,500 yr B.P.; while that at depth of 300 cm was outerpolated as 14,000 yr B.P. based on the average sedimentary rate of 25 cm/ky at the core interval of 200 to 250 cm.

During the last glacial maximum, the sea level of the east area of China had been -150 to -160 m and the sea level began to rise very quickly after 15,000 yr B.P. (Zhao *et al*, 1979). According to our data, there is no fresh-water microfossils found from the bottom of the core. Therefore, this core was deposited after the stage of the sea-level rising, suggesting that the bottom sediment may not be older than 18,000 yr B.P.

4-4-2. Foraminiferal assemblages in core 97-02

One hundred and twenty-nine benthic and twenty planktonic foraminifera species or subspecies are recognized (Appendixes 4-1 and 4-2). The most abundant benthic species (>15%) in the core are *Elphidium magellanium*, *Bolivina robusta* and *Ammonia beccarii* var.; the common species (5-15%) include *Elphidium advenum*, *Quinqueloculata vulgaris*, *Florilus decorus*, *Cassidulina carinata*, *Ammonia kienziensis*, *Pararotolia nipponica*, *Bulimina marginata*, *Epistominella naraensis*, *Cribrononion subincertum*, *Gyroidina nipponica* and *Ammonia compressiuscula* in order (Table 4-2).

Table 4-2. The most abundant and common benthic foraminifera species in core 97-02

type	species	peak abundance and depth
abundant (more than 15% at least in one sample)	*Elphidium magellanium*	43.2% in 380 cm
	Bolivina robusta	36.1% in 60 cm
	Ammonia pauciloculina	18.1% in 0 cm
	Ammonia beccarii	17.8% in 290 cm
common (5-15% at least in one sample)	*Elphidium advenum*	13.8% in 460 cm
	Quinqueloculata vulgaris	13.4% in 210 cm
	Florilus decorus	12.0% in 10 cm
	Cassidulina carinata	9.7 % in 150 cm
	Ammonia kienziensis	7.8% in 0 cm
	Pararotalia nipponica	7.7% in 270 cm
	Bulimina marginata	7.4% in 50 cm
	Epistominella naraensis	6.9% in 0 cm
	Cribrononion subincertum	6.0% in 320 cm
	Gyroidina nipponica	5.3% in 20 cm
	Ammonia compressiuscula	5.1% in 110 cm

Benthic foraminifera consist of three kinds of species according to their modern distribution in the surface sediments of the East China and Yellow Seas (Wang *et al.*, 1985a, Wang *et al.*, 1985b; Wang *et al.*, 1985c; Wang *et al.*, 1988). Assemblage A species (including two sub-assemblages with the boundary of 20 m in water depth, especially in the Yellow Sea) mostly occur the coastal water and inner shelf water (water depth less than 40-50 m), such as *Ammonia beccarii* var. (including *A. beccarii*, *A. tepida*, and *A. limbatobeccarii*), *Ammonia convexdorsa*, *Elphidium magellanicum*, *Florilus decorus*, *Cribrononion vitreum*, *Elphidium advenum*, *Buccella frigida*, *Cribrononion subincertum* and *Pararotalia nipponica*. Assemblage B species are often found in the middle shelf with water depths between 50-100 m, such as *Ammonia compressiuscula*, *Ammonia Ketienziensis angulata*, *Bolivina robusta*, *Bulimina marginata*, *Astrononion tasmanensis*, and *Hanzawaia nipponica*. Assemblage C species, such as *Cassidulina carinata*, *Globocassidulina subglobosa* and the Lagenids, mostly live in the outer shelf where the water depth is more than 100 m.

The assemblage A appears mainly in the lower part (510-150 cm) of core 97-02, while the assemblages B and C dominate the upper part (300-0 cm) of the core (Fig. 4-3). These species are mainly controlled by water depth, connected with the influence of the water masses.

The planktonic foraminifera assemblage is mainly composed of *Globigerinoides ruber*, *G. sacculifer*, *Neogloboquadrina dutertrei*, *Globigerinita glutinata*, *Globigerina bulloides*, *G. calida*, and *Pulleniatina obliquiloculata* (Appendix 4-2). They are the species mostly occurring in the temperate water of the north Pacific (Be, 1977). Compared with the core 255 of the southern Okinawa Trough (Li *et al*, 1997), core 97-02 has more left-coiled *Neogloboquadrina pachyderma* (up to 14.3%) due to a generally colder surface water while the left-coiled species could be barely seen in core 255. Only the *Pulleniatina obliquiloculat* displays an apparent variation boundaries at the core depths of 300 and 200 cm and a well correlation with that of core 255 (shown in Fig. 4-2).

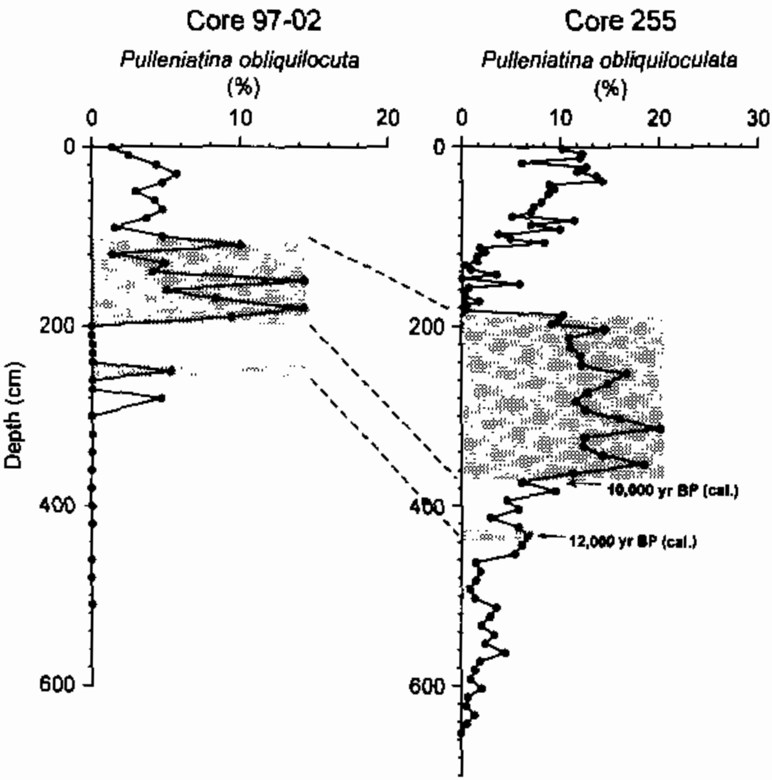

Figure 4-2. Stratigraphy and correlation of core 97-02 and core 255 from the southern East China Sea (after Li et al., 1997)

The chronology at depth of 200 and 250 cm in core 97-02 is correlated to the ages 10,000 cal.yr BP (370 cm) and 12,000 cal. yr BP (430 cm) in core 255

4-3. Down-core variations of benthic foraminifera

Benthic foraminifera are mostly controlled by the water depth in the East China Sea and Yellow Sea areas (Wang *et al.*, 1988). Their modern distribution ecology provide bases for the reconstruction of paleo-water depth during the late Quaternary. Here are their down-core variations in core 97-02 (Fig. 4-3):

Ammonia beccarii var. distributes mostly in the water less than 50 m in the East China Sea, while it reflects a coastal water within 20 m in the Yellow Sea. In a low salinity swamp, its content can sometimes reach more than 90% (Hong, 1982). In core 97-02, *A. beccarii*, *Pararotalia nipponica*, *Elphidium magellanicum* and *Cribrononion subincertum* percentages have the similar down-core variation trend: a high value at depth of below 300 cm (average 13.1%, 6.4%, 32.6%, 2.9%, respectively), medium-to- low value at the core interval of 150-250 cm (average 2.6%, 2.8%, 11.9%, 1.0%, respectively), and almost bare in the top 150 cm, which implies a water depth change at the core depths of 150 and 300 cm below 300 cm, the water depth was much shallow about 0-20 m; above the core depth of 300 cm, the water might become deeper and deeper; and then above the core depth of 150 cm, the water was deeper than 50 m.

Elphidium advenum is often seen in all the shelf of the East China Sea and more in the inner shelf (Wang *et al.*, 1988). It gradually decreases from about 10% at the bottom to about 2% at the top of the core, which implies that the water depth became deeper gradually.

Ammonia compressiuscula is most abundant in the middle-shelf with water depths of 50-100 m, but in the Yellow Sea, it has a high percentage in water of 20-50 m where the Yellow Sea cold water dominates (Fig. 4-1). *A. compressiuscula* and *Astrononion tasmanensis* have the same down-core variations: at the core depth below 300 cm, there are a low value (average 1.2 and 0.7%, respectively), and a relatively high value at the upper part of the core

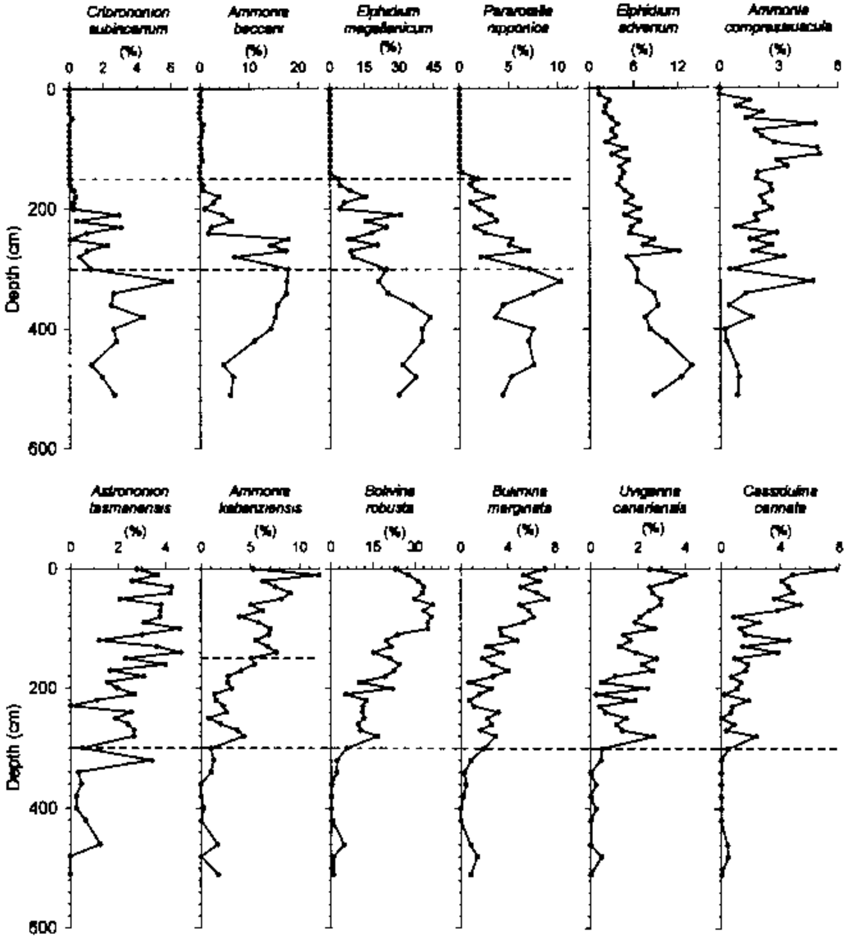

Figure 4-3. Down-core variations of benthic foraminifera in core 97-02

(average 2.3 and 2.8%, respectively). This change reflects that the core interval above 300 cm had the water depth of more than 20 m, while that below 300 cm contained a water depth less than 20 m.

Ammonia ketienziensis angulata distributes in the water deeper than 20 m, but it is very abundant in water deeper than 50 m, and becomes the domain species of Yellow Sea cold water together with *Astrononion tasmanensis*. In core 97-02, its change shows two steps: from average 0.7% below the core depth of 300 cm, to average 3.0% at the core interval of 300-150 cm and to average 6.9% above the core depth of 150 cm, which implies that the core depths of 300 cm and 150 cm are the boundaries of paleo-water depths of 20 and 50 m, respectively.

Bolivina robusta, Bulimina marginata, Uvigerina canariensis and *Cassidulina carinata* have the same trend in the down-core variation. They have a very low value (almost zero) below the core depth of 300 cm and increase gradually in the upper part up to 40, 7, 4 and 8%, respectively. These deeper water species increase in the upper part of the core, reflecting the deepening of water depth

4-4. Paleo-water depth reconstruction of core 97-02

The down-core variations of benthic foraminifera species shown above have exhibited the changes of the paleo-water depth. From around shallower than 20 m (at the core interval of 510-300 cm), to about 20-50 m (at the core interval of 300-150 cm) and to about 50-100 m (at the core interval of 150-0 cm). This can also be indicated by other evidences.

The absolute abundances of both benthic and planktonic foraminifera have a trend to increase sharply when water becomes deeper in the shelf (Wang *et al.*, 1985c). Both benthic and planktonic foraminiferal abundances of core 97-02 also show a rapid down-core change from a few to several thousands specimens per gram of dried sediment from bottom to surface of the core. The ratio of planktonic to total foraminifera also increases from a few to about 40 percent at the same time (Fig. 4-4 and Appendix 4-3). All these indicate that the paleo-water depth of core 97-02 has become deeper after the last glacial maximum.

Benthic foraminifera can be subdivided into six groups according to the test component, forming of wall crystals, and arrangement of chambers: the agglutinated, the porcelaneous, the Lagenids, the serial hyaline, the planispiral hyaline, and the trochospiral hyaline. In the East China Sea, the inner shelf is dominated by the trochospiral and planispiral hyaline groups, while the deeper area of middle-outer shelf is mostly made up of the serial hyaline group; And the Lagenids dominate much deeper area like the slope and the trough (Wang *et al.*, 1985c). The planispiral and serial groups are the main types of benthic foraminifera and have a large variation through the core. Figure 5 shows down-core variations of both groups. We can see that the serial group increased above the core depth of 300 cm (from 13.5 to 51.5%), while the planispiral group increased below the core depth of 150 cm (from 20.8 to 58.7%), which implies that the water depth of this location becomes deeper above the core depth of 300 cm and much deeper above the core depth of 150 cm.

On the basis of the above analysis, we think that the most striking changes in the shelf environment of the East China Sea is the paleo-water depth. The paleo-water depth became deeper and deeper from the bottom to the top of core 97-02. At the core interval of 510-300 cm (before 14,000 yr B.P.), the water was much shallower than 20 meters, like the modern coastal area with high percentage of *Ammonia beccarii* and a very high percentage of planispiral hyaline benthic foraminifera; and then at the core interval of 300-150 cm (about 14,000-7,500 yr B.P.), it became deeper about 20-50 meters (inner shelf) which was indicated by the still high content of planispiral hyaline benthic foraminifera; and at the core interval of 150 to 0 cm (after 7,500 yr B.P.), the paleo-environment was much like the modern middle shelf area, with 50-100 m water depths and higher percentage of the serial hyaline benthic foraminifera.

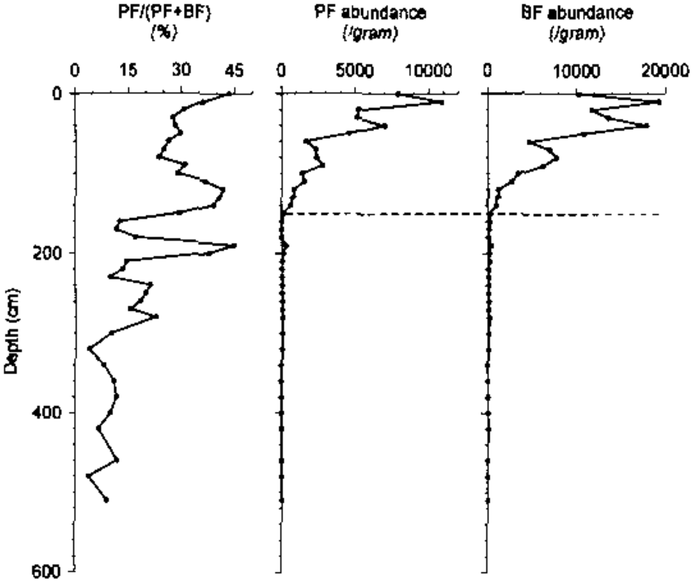

Figure 4-4. Down-core variations of the foraminiferal abundances and planktonic foraminiferal pencentage

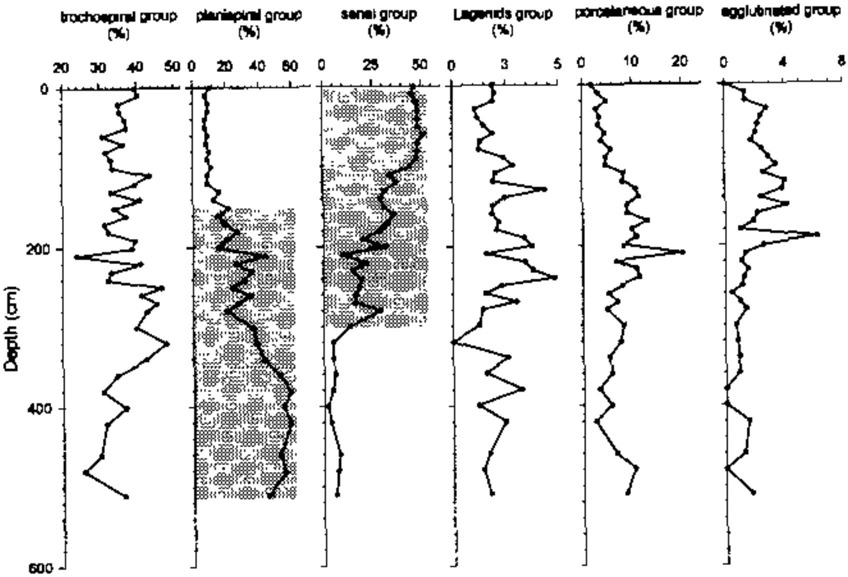

Figure 4-5. Down-core variations of six groups of benthic foraminifera in core 97-02

4-5. Discussion

Planktonic and some typical benthic foraminifera species are good indicators of the paleo-water temperature and water masses (Figs. 4-2 and 4-6). The water was cold during the period of lower sea-level because the benthic foraminifera were mainly composed of cold water species (at the core interval of 510-300 cm) ; The water began to get warmer after 14,000 yr B.P. (above the core interval of 300 cm), which was indicated by the increase of some warm water benthic species *Lenticulina* spp., *Hyalina balthica*, and *Ammonia pauciloculata*. However, it might be still cold because the cold water benthic species *Buccella frigida* (Wang *et al.*, 1988) shows a relatively high percentage at the core interval of 300-150 cm (about 14,000-7,500 yr B.P.), and the water mass dominating this area was mostly similar to the modern Yellow Sea cold water. After 7,500 yr B.P., the water temperature becomes warmer (it may be the warmest since the last glacial), which was reflected by the lowest percentage of cold water species (*Buccella frigida*) and the highest percentages of warm water species (*Lenticulina* spp., *Hyalina balthica* and *Ammonia pauciloculata*).

The planktonic species *Pulleniatina obliquiloculata*, an indicator of Kuroshio Current, has often been regarded as a characteristic species of warm and high salinity water (Thompson, 1981; Wang *et al.*, 1985c; Chinzei *et al.*, 1987; Oda and Takemoto, 1992; Li *et al.*, 1997). Its abundance increases apparently above the core depth of 300 cm, especially above 200 cm, which implies that a certain warm water mass existed (such as the Yellow Sea Warm Current or the "outer-shelf water of the East China Sea") and affect this area strongly after 10,000 yr B.P. (above the core depth of 200 cm), though it had begun to get warm since approximately 14,000 yr B.P. (at the core depth of 300 cm).

It is thought that the warm current began to have a stronger influence in the study area

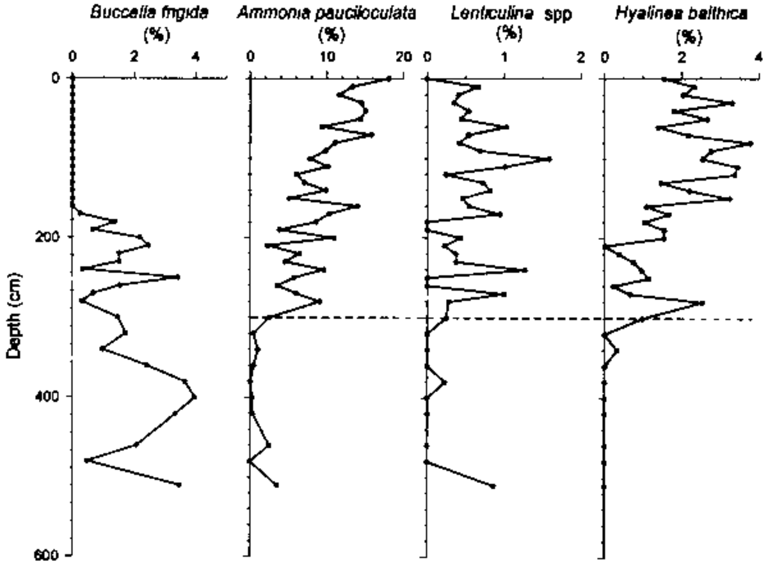

Figure 4-6. Down-core variations of water temperature-indicated species

by the post-glacial westward shift of the Kuroshio Current. Jian *et al.* (1998) interpreted that the Kuroshio Current entered the Okinawa Trough thoroughly at about 7,000 years ago. For further comparison of the current changes of the East China Sea, we need the detailed AMS ^{14}C dates of core 97-02.

The species diversity change of benthic foraminifera is shown in Figure 7. The relatively higher diversity [H(S)] for benthic foraminifera is shown at the core interval of 300 to 100 cm. This coincides with the high simple species diversity (S, number of the species in each sample) at this interval, which reflects its adaptation to the environment of the deeper inner and middle shelves.

According to changes of the agglutinated group and *Textularia* spp., there is an increase above the core depth of 200 cm, which may inform the high-energy coastal environment in the lower part of the core. The high energy of sea water prevents the formation and preservation of agglutinated test. This is also supported by the high coarse fractions at this interval (Fig. 4-7) and severe abrasion of large foraminifera specimens or mollusca shells observed during the proceeding of foraminifera samples.

4-6. Conclusions

Core 97-02 of the northern East China Sea may disclose the strata after the last glacial maximum and shows evident paleoceanographic changes. The foraminifera assemblages reflect that the water depth deepens from about 0-20, to 20-50 and to 50-100 m at the core depths of 510-300, 300-150 and 150-0 cm, respectively. At the same time, the absolute abundances of both planktonic and benthic foraminifera increase rapidly from a few to several thousands. The planktonic ratio in total foraminiferal fauna increases from a few to 40 percent with the

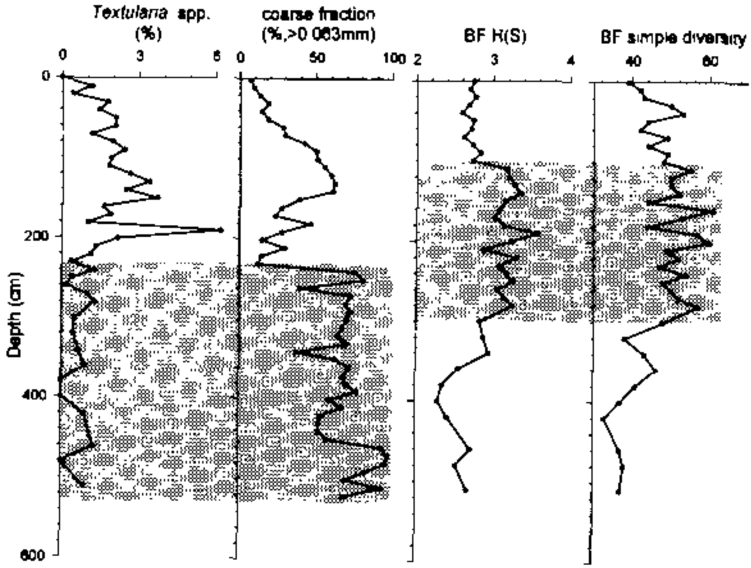

Figure 4-7. Down-core variations of benthic foraminifera species diversity, *Textularia* spp. and coarse fraction (>0.063mm) in core 97-02

increase of water depth

Characteristic species of both benthic and planktonic foraminifera show that the water temperature has increased on account of the enhancement of warm water mass (such as the Yellow Sea Warm Current), and the weakening of both the Yellow Sea cold water and the coastal water in this area since the last glacial. The Yellow Sea Warm Current might finally dominated this area very strongly after 10,000 yr B.P. (above the core depth of 200 cm) though it had come to affect this area since 14,000 yrs B.P. (above the core depth of 300 cm), with the post-glacial westward shift of the Kuroshio Current.

Temperature-indicated species also shows that the water temperature began to increase after 14,000 yr B.P and reach the highest after 7,500 yr B.P., which may reflect the thorough entering of the Kuroshio Current into the East China Sea at that time

REFERENCES

Anderson, J.B., 1975a: Ecology and distribution of foraminifera on the Weddell Sea of Antarctic. *Micropaleontology*, 21: 69-96.

Anderson, J.B., 1975b: Factors controlling $CaCO_3$ distribution in the Weddell Sea from foraminiferal distribution battens. *Marine Geology*, 19: 315-332.

Anderson, J.B. and B.F. Molnia, 1989. Glacial-Marine Sedimentation American Geophysical Union short Course Geology 9, 149pp.

Archer, D., M. Lyle, K. Rodgers, and P. Froelich, 1993. What controls opal preservation in tropical deep-sea sediments? *Paleoceanography*, **8**: 7-21.

Aspila, K.I., H. Agemian, and A.S.Y. Chau., 1976. A semi-automatic method for the determination of inorganic, organic, and total phosphate in sediments. *Analyst*, **101**. 187-197.

Baker P.F. and D.H. Griffith, 1972. The evolution of the Scotia Ridge and Scotia Sea. *Phil. Trans. Royal Soc. London*, **271**: 151-183.

Bakker, P.F. and I.W.D. Dalziel, 1983. Progress in geodynamics of the Scotia Arc regions. In: Geodynamics of the Eastern Pacific region, Caribbean and Scotia arcs. Geodynamics Series 9, edited by S.J.R. Cabre

Be, A.W. H., 1977: An ecological, zoogeographic and taxonomic review of recent planktonic foraminifera. In: A.T. S. Ramssy(ed.), Oceanic Micropaleontology, Vol. 1. Academic Press, London, pp.105-149.

Berger, W.H., 1967: Foraminiferal ooze: solution at depths. *Science*, 156: 383-385.

Berger, W.H., V.S. Smetacel, and G. Wefer, 1989. Ocean productivity and paleoproductivity – an overview. In: Productivity of the Ocean: Present and Past, edited by W.H.

Berger, V.S. Smetacet, and G. Wefer, John Wiley & Sons, Bernhard.

Berner, R.A., 1982. Burial of organic carbon and pyrite sulfur in the modern ocean: its geochemical and environmental significance. *Am. J Sci.*, **278**: 451-473

Berner, R.A., 1984. Sedimentary pyrite formation: an update. *Geochim. Cosmochim Acta*, **48**: 605-615.

Berner, R.A. and R. Raiswell, 1984. C/S method for distinguishing freshwater from marine sedimentary rocks. *Geology*, **12**: 365-368.

Berner, R.A. and J.T. Westrich, 1985. Bioturbation anf the early diagenesis of carbon and sulfur. *Am. J. Sci.*, **285**: 193-206.

Bjorck, S., Hakansson, H., Zale, R., Karlen, W. & Jonsson, B.L., 1991: A late Holocene lake sediment sequence from Livingston Island, South Shetland Islands, with palaeoclimatic implications. *Antarctic Science*, 3: 61-72.

Bjorck, S., Hannelore H., Siv, O., Lena, B. & Jan J., 1993: Paleoclimate studies in South Shetland Islands, Antarctica, based on numerous stratifraphic variables in lake sediments. *Journal of Paleocliamnology*, 8: 233-272.

Boltovskoy E. & Wright, R., 1976: Recent Foraminifera. Dr. W Junk B.V.-The Hague. 515pp., 133 figs.,17 tables.

Bruchert, V. and L.M. Pratt, 1996. Contemporaneous early diagenetic formation of organic and inorganic sulfur in estuarine sediments from St. Andrew Bay, Florida, USA. *Geochim. Cosmochim. Acta*, **60**: 2325-2332.

Brzezinski, M.A., 1985. The Si/C/N ratios of marine diatoms: interspecific variability and the effect of some environmental variables. *J. of Phycology*, **21**: 345-357.

Calvert, S.E., 1987. Oceanographic controls on the accumulation of organic matter in marine sediments. In: Marine Petroleum Source rocks, Geological Society Special Publication No. 26, edited by J. Brooks and A.J. Fleet.

Chang, S.K., Choi, J.Y. & Je, J.G., 1988: Eastern Beach sediments of Fildes Peninsula King Georrge Island, South Shetland, Antarctic. *Journal of Korean Earth Science Society*, 9: 1113-122. (in Korean, with English abstract)

Chen Chin, 1966: Calcareous Zooplankton in the Scotia Sea and Drake passage, *Nature*, 212(5063): 678-681.

Chen Ronghua and Zhan Yufen, 1991: Microfossils iu the sediments. Report on the sedimentation and investigation on the Great Wall Cove, Antarctica, pp. 76-86.

Chinzei, K., Fujioka, K., Kitazata, H., Koizum, T., Oda, M., Pkada, H., Sakai, T. & Tanimura, Y., 1987. Post-glacial environmental changes of the Pacific Ocean off the coast of central Japan. *Marine Micropaleontology*, 11: 273-291.

Compton, J.S., D.A. Hodell, J.R. Garrido, and D.J. Mallinson, 1993. Orgin and age of phosphorite from the south-central Florida Platform: Relation of phosphogenesis to sea-level fluctuations and $\delta^{13}C$ excursions. *Geochim. Cosmochim. Acta*, 57: 131-146Chang, S.K. & Yoon, H.I., 1995: Foraminiferal assemblages from bottom sediments at Marian Cove, South Shetland Islands, West Antarctica. *Marine Micropaleontology*, 26: 223-232.

Crespin, I., 1960: Some recent foraminifera from Vestford Hills, Antarctic. *Science reports of Tohoku University*, 2nd serious(Geology). Special volume 4: 19-31.

Dean, W.E. and M.A. Arthus, 1989. Iron-sulfur-carbon relationships in organic-carbon-rich sequences, I. Cretaceous Western Interior seaway. *Am. J. Sci.*, **289**: 708-743.

Domack, E.W., T.A. Mashiotta, and L.A. Burkely, 1993. 300-year cyclicity in organic matter preservation in Antarctic fjord sediments. In: The Antarctic Paleoenvironment. A Perspective on Global Change Antarctic Research Series v. 60, edited by J. Kennett and D. Warnke.

Domack, E.W., Jull, A.J.T., Anderson, J.B., Linick, T.W. and Williams, C.R., 1989:

Application of Tandem Accelerator Mass Spectrometer dating to late Pleistocene-Holocene Sediments of the East Antarctic continental shelf. *Quaternary Research*, 31:277-287.

Domack, E.W. & McClennen, C.L., 1996: Accumulation of Glacial Marine sediments in fjords of the Antarctic Peninsula and their use as late Holocene Paleoenvironmeantal indicators. *Antarctic Research*, Series 70: 135-154.

Echols, R. J., 1971: Distribution of the foraminifera in sediments of the Scotia Sea area, Antarctic waters. *Antarctic Research*, Serious 15:93-168.

Ferdelman, T.G., T.M Church, and G.W. Luther III, 1991. Sulfur enrichment of humic substances in A Delaware salt marsh sediment core *Geochim Cosmochim. Acta,* **55**: 979-988.

Filippelli, G.M. and M.L. Delaney, 1994. The oceanic phosphorus cycle and continental weathering during the Neogene. *Paleoceanography*, 9: 643-652.

Fillon, R. H., 1974: Late Cenozoic foraminifera paleocology of the Ross Sea, Antarctic *Micrapaleantology*, 20(2): 129-151.

Finger, K. L. and Lipps, J. H., 1981: Foraminifera decimation and repopulation in an active volcanic calendera, Deception Island, Antarctic. *Micropaleontology*, 27: 111-139.

Francois R., 1987. A study of sulfur enrichment in the humic fraction of marine sediments during early diagenesis. *Geochim Cosmochim Acta*, **51**: 17-27.

Frenzel, B., Pecsi, M. and Velichko, A.A., 1992. Atlas of Paleoclimates and Paleoenvironments of the Northern Hemisphere, Late Pleistocene-Holocene. Geogr. Res. Inst., Hung. Acad. Sci., Budapest. 153 pp.

Gibson, T. G. and Buzas M.A., 1973. Species diversity: patterns in modern and Miocene foraminifera of the eastern margin of North America. *Geological Society of America Bulletin*, **84**: 217-238.

Gordon, A. and W. Nowlin, 1978 The basin waters of the Bransfield Strait. *J Phys Oceanogr.*, 8: 258-264.

Griffith, T.W. and Anderson, J.B., 1989: Climate control on sedimentation in Bays and fjords of the northern Antarctic Peninsula. *Marine Geology*, 85: 181-204.

Grobe, H. & Mackensen, A., 1992: Late Quaternary climatic cycles as recorded in sediments from the Antarctic continental margin. *Antarctic Research*, Series 56: 349-376.

Grobe, H., Mackensen, A., Hubberten, H.-W., SpieB, V., and Rutterer, D. K., 1990: Stable isotope record and late Quaternary sedimentation rates at the Antarctic continental margin. In: Bleid, U., and Thied, J.(Eds.), Geological Histry of the Polar Oceans: Arctic versus Antarctic. Kluwer Academic Pub., pp 539-572.

He, Yan, Hu, L. and Wang, K., 1965. Quaternary Foraminifera from northern Jiangsu. *Mem Inst Geol., & Paleont. Acad. Sinica*, 4:51-162 (in Chinese, with Russian Abstract)

Hemleben, C., Spindler, M. and Anderson, O.R., 1988. Modern Planktonic Foraminifera Springer, New York. 363pp.

Herb, R., 1971: Distribution of recent benthonic foraminifera in the Drake Passage. In: G. A. Llano and I. E. Wallen (Eds.), Biology of the Antarctic Seas IV. *American Geophysical Union, Antarctic Reseach*, serious 17: 251-300.

Hjort, C., Ingolfsson, O., & Bjorck, S., 1992: The last major deglaciation in the Antarctic Peninsula regin - A review of recent Swedish Quaternary research. In: Y. Yoshida (ad.), Recent Progress in Antarctic Earth Science. Terra Scientific Publishing Company, Tokyo.

Hong, Xueqing, 1982. Distribution of Foraminifera in the Sea Shore of the East China Sea and the Yellow Sea, and Its Geological Significance. M Sci. thesis, Tongji University, Shanghai. 60 pp.

Hong, S.M., Park, B.K., Yoon, H.I., Kim, Y.D. and Oh J.K , 1991: Depositional environment in and paleoglacial setting ground Marian Cove, King George Island, Antarctic. *Korean Journal of Polar Research*, 2: 73-85. (in Korean, with English abstract)

Howard, W.R. and W.L. Prell, 1994. Late Quaternary $CaCO_3$ production and preservation in the Southern Ocean: implications for oceanic and atmospheric carbon cycling. *Paleoceangr.*, **9**: 453-482.

Huntley, M., D.M. Karl, P. Niler, and O. Holm-Hansen, 1991. Research on Antarctic Coastal Ecosystem Rates (RACER): an interdisciplinary field experiment. *Deep-Sea Res.*, **38**: 911-941.

Inglolfsson O., Hjort, O., Bjorck, S. & Smith, R.I.L., 1992: Late Pleistocene and Holocene Glacial history of James Ross Island, Antarctica. *Boreas*, 21: 209-222.

Jacobs, S.S. and J.C. Comiso, 1993. A recent sea-ice retreat west of the Antarctic Peninsula. *Geopy. Res. Lett.*, **20**: 1171-1174.

Jeffers, J.D. and J.B. Anderson, 1990. Sequence stratigraphy of the Bransfield Basin, Antarctica: Implications for tectonic history and hydrocarbon potential. In: Antarctica as an Exploration Frontier – Hydrocarbon Potential, Geology, and Hazards, edited by B. St. John, American Association of Petroleum Geology Studies Geology 31.

Jian, Zhimin, Li, B., Pflaumann, U., and Wang, P., 1996. Late Holocene cooling event in the western Pacific. *Science in China*(D), 39(5). 522-532.

Jian, Zhimin, Saito, Y., Wang, P., Li, B. and Chen, R., 1998. Shifts of the Kuroshio axis over the last 20,000 years. *Chinese Science Bulletin*. (in press)

John, B.S., 1972: Evidence from the South Shetland Islands towards a glacial history of west Anatarctica. In: D.E. Sugden & R.J. Price (eds.), Polar Geomorphology, Institute of British Geographers, pp.75-92.

Kalin, R., M. Lyle, and R. Zahn, 1992. Carbonate variations in the northeast Pacific during the late Quaternary. *Paleoceangr.*, 7: 43-61.

Keller, R.A., M.R. Fisk, W.M. White, and K. Birkenmajer, 1991 Isotopic and trace element constraints on mixing and melting models of marginal basin volcanism, Bransfield Strait, Antarctica. *Earth Planet. Sci Lett.*, **111**: 287-303.

Kennett, J.P., 1966. Foraminiferal evidence of a shallow calcium carbonate solution boundary, Ross Sea, Antarctic. *Science*, 153: 191-193.

Kennett, J.P., 1967: New foraminifera from the Ross Sea, Antarctica. *Contributions from the Cushman Foundation for Foraminifera Research*, 18(3): 133-135, pl 11

Kennett, J.P., 1968: The fauna of the Ross Sea: Ecology and distribution of foraminifera, part 6. *New Zealand Department Scientific & Industrial Research Bulletin*, 186: 48pp.

Kim. D. 1996. Biogeochemical cycling of carbon, phosphorus, and silica in California continental slope sediments. Ph.D. Diss., University of California, San Diego.

Kim, D., B.-K. Park, H.I. Yoon, and C.Y. Kang. 1998. Geochemical evidences on the Holocene paleoclimatic changes in Maxwell Bay of South Shetland Islands, West Antarctica. *Geoscience J.*, submitted.

KORDI, 1995. The studies on Natural Environment and Conservation of Antarctica. BSPN 0025-822-7, 846pp.

KORDI, 1996. Antarctic marine geological prospecting report. BSPG00252-935-7, 280pp.

Leinen, M., D. Cwienk, G.R. Heath, P.E. Biscaye, V. Kolla, J. Thiede, and J.P. Dauphin, 1986. Distribution of biogenic silica and quartz in recent deep-sea sediments. *Geology*, 14: 199-203.

Leventhal, J.S., 1983. An interpretation of carbon and sulfur relationship in Black Sea sediments as indicators of environments of deposition. *Geochim Cosmochim. Acta*, 47: 133-137.

Leventer, A., E.W. Domack, S.E. Ishman, S. Brachfeld, C.E. McClennen, and P. Manley, 1996.

Productivity cycles of 200-300 years in the Antarctic Peninsula region: Understanding linkages among the sun, atmosphere, oceans, sea ice, and biota. *Geol. Soc. Am. Bull.*, 108: 1626-1644.

Leynaert, A., D.M Nelson, B. Queguiner, and P. Treguer, 1993. The silica cycle in the Antarctic Ocean: is the Weddell Sea atypical? *Mar. Ecol. Prog. Ser.*, 96: 1-15.Li, Baohua, 1997. Study on the Paleoceanography of the Nansha Area, Southern South China Sea since the Last 700,000 Years. Ph D. thesis, Nanjing Institute of Geology and Paleontology, Academia Sinica, Nanjing. pp.1-99.

Li, Baohua , Jian, Z. & Wang, P., 1997. *Pulleniatina obliquiloculata* as paleoceanographic indicator in the southern Okinawa Trough during the last 20,000 years. *Marine Micropaleontology*, 32(1997): 59-69.

Li, Baohua, *et al.*. Post-glacial paleoceanographic changes in the East China Sea and influence to the climate of adjacent areas. (In preparation)

Li, Y. and Zhang, Q., 1986: Recent foraminifers from Great Wall Bay King George Islands, Antarctic. *Acta Micropaleontologica Sinica*, 3: 335-346. (in Chinese, with English abstract)

Li, Y. and Li, B., 1996: Late Pleistocene Foraminifera in the Fildes Peninsula of King George Island, Antarctica. *Acta Micropaleontologica Sinica*, 13(3): 255-260. (in Chinese, with English abstract)

Lipps, J. S. and Krebs, W. N., 1974: Planktonic foraminifera associated with Antarctic sea ice *Journal of Foraminifera Research*, 4: 80-85.

Mackensen, A., Grobe, H., Kuhn, G. & Futterer, D.K., 1990: Benthic foraminiferal assemblages from the eastern Weddell Sea between 68 and 73 symbol 176 \f "Symbol" \s 10.5□□S: Distribution, ecology and fossilization potential. *Marine Micropaleontology*, 16: 241-283.

Mausbeacher R., Muller, J., Munnich, M. & Schmidt, R., 1989: Evolution of postglacial sedimentation in Antarctic lakes (King George Island) *Zeitschrift fur Geomorphologie N F*, 33: 219-234.

Milam, R. W. and Anderson, J. B., 1981: Distribution and ecology of recent benthonic foraminifera of the Adelie-George V continental shelf and slope, Antarctica. *Marine Micropaleontology*, 6: 279-325.

Min, Qiubao & Wang, P., 1979. Quaternary transgression in Shanghai region. *Journal of Tongji University*, 2: 109-118 (in Chinese, with English abstract)

Nomura, R, 1983: Foraminifera from the raised beach deposits on the east coast of Luzow-Holm Bay, Antarctica. *National Institute Polar Research, Memorial*, special issue 28: 219-228.

Morse, J.W. and K.C. Emeis, 1990. Controls on C/S ratios in hemipelagic upwelling sediments *Am. J. Sci.*, 290: 1117-1135.

Mortlock, R.A. and P.N. Froelich, 1989. A simple method for the rapid determination of biogenic opal in pelagic marine sediments. *Deep-Sea Res.*, 9: 1415-1426.

Mossmann, J.R , A.C. Aplin, C.D. Curtis, and M.L. Coleman, 1991. Geochemistry of inorganic and organic sulphur in organic-rich sediments from the Peru Margin. *Geochim Cosmochim Acta*, 55: 3581-3595.

Niler, P.P., A. Amos, and J.-H. Hu, 1991. Water masses and 200 m relative geostrophic circulation in the western Bransfield Strait region. *Deep-Sea Res.*, 38: 943-959.

Oda, M. and Takemoto, A., 1992. Planktonic foraminifera and paleoceanography in the domain of the Kuroshio Current around Japan during the last 20,000 years. *Quaternary Research*, 31(5): 341-357.

Osterman, L. E. and Kellogg, T.B., 1979: Recent Bentic foraminiferal distributions from the Ross Sea, Antarctica: Relations to ecologic and oceanographic conditions. *Journal* *of Foraminifera Research*, 9: 250-269.

Park, B.K., Yoon, H.I., Woo, H.J., Lee, K.S., Bark E.-J. and South, J., 1995: Late Holocene Paleoceanography from Core Sediments in the Admiralty Bay and Maxwell Bay, King George Island, Antarctica. *The Journal of the Korea Society of Oceanography*, 30(4): 302-319. (in Korean, with English abstract)

Pflum, C. E., 1966: The distribution of foraminifera in the eastern Ross Sea, Amundsen Sea, and Bellingshausen Sea. *Antarctic Bulletin of American Paleontology*, 50: 151-209.

Qin, Yunshan & Zhao, S., 1986. A sedimentary model of China shelf and the problem of shelf transgression since the late Pleistocene. In: International Geological Correlation Program Project No.200 China National Working Group (Editor), China Sea Level Changes. China Ocean Press, Beijing. pp.12-26. (in Chinese, with English abstract)

Raiswell, R. and R.A. Berner, 1985. Pyrite formation in euxinic and semieuxinic sediments. *Am J. Sci.*, **285**: 710-724.

Rao, P.S., Mascarenhas, A., Paropkari, A.L., and C.M. Rao, 1994. Organic carbon-sulfur relatioships in sediments cores from the western and eastern continental margins of India. *Mar. Geol.*, 117: 227-236.

Rea, D.K., N.G. Pisias, T. Newberry, 1991. Late Pleistocene paleoclimatology of the Central Equatorial Pacific: flux patterns of biogenic sediments. *Paleoceangraphy*, 6: 227-244.

Redfield, A.C., Ketchum, B.H. and Richards, F.R., 1966: The influence of organism on the composition of sea water. In: M.N. Hill (General Editor), The Sea: Ideas and Observations on Progress in the study of the Seas. Interscience Publishers, pp.26-77.

Ruttenberg, K.C. and R.A. Berner, 1993. Authigenic apatite formation and burial in sediments from non-upwelling, continental margin environments. *Geochim. Cosmochim. Acta*, 57: 991-1007.

Setty, M. G.A.P., Williams , R. and Kerry, K.R., 1980: Foraminifera from the Deep lake terraces, Vetford Hills, Antactic. *Journal of Foraminifera Research*, 10: 303-312.

Sugden D.E & C.M. Clapperton, 1986: Glacial history of the Antarctic Peninsula and South Georgia. *South African Journal of Sciences*, 82: 508-509.

Tang, Baogen, 1996. Quaternary stratigraphy in the shelf of the East China. In: Yang, Zigeng & Lin, Hemao (editors), Quaternary Stratitgraphy in China and Its International Correlation. Geological Publishing House, Beijing. pp. 56-75. (in Chinese)

Thompson, P.R. 1981. Planktonic foraminifera in the north Western Pacific during the last 150,000 years: comparison of modern and fossil assemblages. *Palaeogeography, Palaeoclimatology, Palaeoecology*, 35: 241-279.

Uchio, T., 1960: Benthic foraminifera of the Antarctic Ocean. *Biological Results of the Japanese Antarctic Research Expedition*, 12: 1-20.

Ujiie, H., Tanaka, Y. and Ono, T., 1991. Late Quaternary paleoceanographic record from the middle Ryukyu Trench slope, northwest Pacific. *Marine Micropaleontology*, 18:115-128.

Van Cappellen, P.V. and E.D. Ingall, 1994. Benthic phosphorus regeneration. Net primary production, and ocean anoxia: A model of the coupled marine biogeochemical cycles of carbon and phosphorus. *Paleoceanography*, 9: 677-692.

Wakeham, S.G., J.S. Sinninghe Damste, M.E.L. Kohnen, and J.W. De Leeuw, 1995. Organic-sulfur compounds formed during early diagenesis in Black Sea sediments *Geochim Cosmochim Acta*, 59: 521-533.

Wang, Pinxian, 1990. The China Seas in ice age--- research results and problems. In: P. Wang, Q. Lao and Q. He (Editors), Proc. First Int. Conf. On Asian Marine Geology. China Ocean Press, Beijing. pp.181-190.

Wang, Pinxian, 1992. West Pacific marginal seas in the last glacial: a paleoceanographic comparison. In: Z. Ye and P. Wang (Editors), Contributions to Late Quaternary Paleoceanography of the South China Sea. Qingdao Ocean University Press, QingDao. pp.308-312. (in Chinese, with English abstract)

Wang, Pinxian, Min Q and Bian, Y., 1985a. Distribution of foraminifera and ostracoda in bottom sediments of the northwestern part of the Southern Yellow Sea and its geological significance In: P. Wang (Editor), Marine Micropaleontology in China. China Ocean Press, Beijing. pp.93-115.

Wang, Pinxian, Zhang, J and Gao, J., 1985b. Microfauna of the lower sea-level stage at the end of Pleistocene from the East China Sea and the Yellow Sea. In: P. Wang (Editor), Marine Micropaleontology in China. China Ocean Press, Beijing. pp. 256-264.

Wang, Pinxian, Zhang, J. and Min, Q., 1985c. Distribution of Foraminifera in surface sediments of the East China sea. In: P. Wang (Editor), Marine Micropaleontology in China. China Ocean Press, Beijing. pp. 34-69.

Wang, Pinxian, Zhang, J., Zhao, Q., Min, Q., Bian, Y., Zheng, L., Cheng, X., and Chen, R., 1988. Foraminifera and Ostracoda in Bottom Sediments of the East China Sea China Ocean Press, Beijing. 438 pp. (in Chinese, with English abstract)

Wang, Pinxian, Bian, Y., Li, B. and Huang, C., 1996. The Younger Dryas in the west Pacific marginal seas. *Science in China* (D), 39(5): 522-532.

Wefer, G., G. Fischer, D.K. Futterer, R. Gersonde, S Honjo, and D. Ostermann, 1990. Particle sedimentation and productivity in Antarctic waters of the Atlantic sector In: Geological History of the Polar Oceans: Artic Versus Antarctic. edited by U. Bleil and J. Thiede, Kluwer Academic Publishers.

Whiticar, M.J., E. Suess, and H. Wehner, 1985. Thermogenic hydrocarbons in surface sediments of the Bransfield Strait. *Nature*, **314**: 87-90.

Woo, H.J, Park, B.K., Chang, H.D., Chang, S.K. and Yoon, H.I., 1996: Late Holocene paleoenvironments of the King George Island, west Antarctica, using benthic foraminifera. *Journal of the Geological Society of Korea*, 32(5): 393-406. (in Korean, with English abstract)

Xu, Xuedong and Oda, M., 1994. The last deglacial in the East China Sea: evidence from planktic foraminifera in two piston cores. Proc. 1994 Sapporo IGBP Symp., Hokkaido Univ., Sapporo Hokkaido, Japan. pp. 488-492.

Yan, Jun and Thompson, P.R., 1991. Paleoceanographic evolution in the Okinawa Trough during the late Pleistocene. *Oceanol. Limnol. Sinica*, 22(3): 264-271. (in Chinese, with English abstract)

Yang, Dayuan, 1986. Tidal level changes near the Changjiang estuary since Holocene. In: international Geological Correlation Program Project No.200 China National Working Group (Editor), China Sea Level Changes. China Ocean Press. pp124-131. (in Chinese, with English abstract)

Yang, Zigeng, Lin, H. and Zhang G., 1996. Quaternary straligraphy in the shelf of the Yellow Sea. In: Z. Yang and H. Lin (Editors), Quaternary stratigraphy in China and its international correlation. Geological Publishing House, Beijing. pp.31-55. (in Chinese)

Yoon, H.I., Han, M.W., Park, B.K., Han, S.J. & Oh, J.K, 1992: Distribution, provenance and dispersal pattern of clay minerals in surface sediments, Bransdield Strait, Antarctica. *Geo-Marine Letters*, 12: 23-227.

Yoon, H.I., Han, M.W., Park, B.K., Oh, J.K. & Chang, S.K., 1994: Depositional environment of near-surface sediments, King George Basin, Bransfield Strait, Antarctica. *Geo-Marine Letters*, 12: 1-9.

Yoon, H.I., 1995. Glacimarine sedimentation patterns of Bransfield Strait and adjoining fjord in

South Shetland Islands, Antarctica: Implications for late Quaternary glacial history Ph.D. Diss., Inha University. Incheon. 273pp.

Yoon, H.I., Han, M.W., Park, B.K., Oh, J.K. & Chang, S.K., 1997: Glacial sedimentation and palaeo-glacial setting of Maxwell Bay and its tributary embayment, Marian Cove, South Shetland Islands, West Antarctica. *Marine Geology*, 140: 265-282.

Zhao, Xitao, Geng, X. and Zhang, J., 1979. Sea level changes in the eastern China since the last 20,000 years. *Acta Oceanologica Sinica*, 1: 269-281. (in Chinese)

Zheng, Shouyi, Cheng, T., Wang, X. and Fu, Z., 1978. The Quaternary Foraminifera of the Dayuzhang irrigation area, Shangdong province, and a preliminary attempt at an interpretation of its depositional environment. *Studia Marina Sinica*, 13: 16-78. (in Chinese, with English abstract).

Appendix 2-1. Foraminifera systematics

Astrononion antarcticus (Parr)
Astrononion echolsi Kennett
Cassidulinoides parkerianus (Brady)
Cassidulinoides porrecta (Heron-Allen & Earland)
Cibicides refulgens Mantfort
Elphidium incertum (Williamson)
Elphidium sp.1
Globocassidulina biora (Crespin)
Globocassidulina crassa rossensis Kennett
Lingulino translucida Heron-Allen & Earland
Miliammina arenacea (Champman)
Nonionella bradii (Champman)
Pullenia subcarinata (d'Orbigny)
Pyrgo pentagonica (d'Orbigny)
Quinqueloculata seminula (Linne)
Rosalina globularis d'Orbigny
Trifarina angulosa (Williamson)
Globigerinita glutinata (Egger)
Neogloboquadrina pachyderma (Ehrenberg) L

Appendix 2-2. BF percentages (%), BF abundance, (BDI), fragmentation, yellow shell percentage, CaCO3(%), TOC(%) and C/N ratio in core A10-08

Depth (cm)	0	5	10	15	20	25	30	35	40	45	50	55	60	65	70	75	80	85	90	100	105
weight (gram)	14.2	12.4	15.8	16.7	14.7	18.0	13.9	15.8	16.7	17.5	20.9	23.8	13.0	18.9	14.7	13.7	19.8	16.8	18.8	21.0	21.6
Globocassidulina biora	94.6	51.9	55.6	78.8	40.9	88.9	81.8	91.1	93.1	95	91.3	85.7	88.6	88.5	80	80.4	78.9	65.2	42.9	50	80
G. crassa rossensis	5.4	13.5	15.3	18.9	36.4	11.1	18.2	8.9		5	1.9	5.2	7.1	7.7	13	16.1	8.3	8.7	14.3		
Elphidium incertum		1.9													2		2.8	6.5		12.5	10
Elphidium sp 1		1.9														1.8	5.5	10.9	14.3	12.5	
Cassidulinoides parkerianus		30.8	29.1	2.3	22.7				6.9		3.9		2.9		5		1.8	8.7			
Quinqueloculata seminula											2.9	7.8	1.4	3.8		1.8	0.9		14.3	25	10
Rosalina globularis												1.3									
Astrononion antarcticus																	0.9				
Glibigerinita glutinata																	0.9				
Pyrgo pentagonica																			14.3		
specimen counted	37	52	189	132	22	9	11	302	58	40	103	77	70	26	100	56	109	46	7	8	10
Simple diversity	2	5	3	3	3	2	2	2	2	2	4	4	4	1	4	4	8	5	5	4	3
Abundance (/gram)	2.6	4.2	12.0	7.9	1.5	0.5	0.8	19.2	3.5	2.3	4.9	3.2	5.4	1.4	6.8	4.1	5.5	2.7	0.4	0.4	0.5
epifauna											2.9	9.1	1.4	3.8		1.8	0.9		28.6	25	10
infauna	100	69	71	98	77	100	100	100	93	100	93	91	96	96.2	95	98	95	91	71	75	90
Agglutinated																					
Porcelaneous											2.9	7.8	1.4	3.8		1.8	0.9		28.6	25	10
Hyaline	100	100	100	100	100	100	100	100	100	100	97.1	92.2	98.6	96.2	100	98.2	99.1	100	71.4	75	90

Appendix 2-2. (continued)

depth (cm)	BDI	Fragmentation (%)	Yellow shell (%)	gravel (%)	sand (%)	silt (%)	clay (%)	coarse	TOC (%)	C/N	CaCO3 (%)
0	0.65	13.5	0	14.29	25.09	24 52	36.09	39.38	0 220	5.273	4.166
5	0.09	17.6	0	0.88	11.38	31.88	55.86	12.26	0 287	4 816	4.788
10	0.34	23.1	0	1.77	14.42	30.55	53.26	16.19	0 216	4.709	4 183
15	0.94	11.6	0	4.08	18.16	29.73	48.02	22.24	0.247	4.873	5.063
20	0.00	17.6	0	0	10.09	32.17	57.74	10.09	0 248	4.494	5.023
25	0.67	11.1	0	1.14	15.76	34.74	48.37	16.9	0 228	5 509	4 855
30	0.18	18 2	0	4.66	13.38	31.74	50.49	18.04	0.204	4.994	4.909
35	0.97	1.3	0	3.5	12.19	30 98	53.33	15.69	0.152	5.038	5 201
40	-0.43	16.7	14.8	4.75	18.81	34.16	42.29	23.56	0.159	5.330	4.821
45	0.63	12.5	0	1.49	26.8	32.62	39 09	28 29	0.071	5.518	4.872
50	0 96	9.4	6.25	9.47	24.87	29.36	36.3	34.34	0.073	4 330	5.067
55	0.91	4.3	0	5.11	36.92	24.79	33 18	42 03	0.113	5.011	4 849
60	1.00	14.9	0	0.84	24.7	32.35	42.11	25.54	0 107	4 963	4 607
65	0.84	8.0	0	35.66	36.22	10.51	17.6	71.88	0.092	5.240	4 871
70	0.85	9.7	0	8.44	19.86	28.47	43.23	28.3	0 148	4.941	4 322
75	0.87	7.4	0	5.11	20.13	28.5	46.25	25.24	0.082	4.150	4.987
80	0 96	14.7	0	2.89	17.33	32 78	47	20 22	0 085	4.705	3.921
85	0.94	17.6	0	6.96	27.5	25.6	39.94	34.46	0 077	5 052	4.083
90	0.67	0.0	0	25.43	36.45	12.51	25.61	61.88	0.029	2.903	4.348
95				32 49	32.93	10 98	23.6	65 42	0 028	3 009	4 736
100	1.00	0 0	0	22.08	36.07	15.06	26.78	58.15	0 039	2 927	4.860
105	1.00	0.0	0	20.31	35.89	15.67	28.14	56.2	0.035	3.516	4 588

Appendix 2-3. BF percentages (%), BF abundance, (BDI), fragmentation, yellow shell percentage, CaCO3(%), TOC(%) and C/N ratio in core A10-01

depth (cm)	0	5	10	15	20	25	30	40	45	50	55	60	65	70	75	80	85	90
weight (gram)	7.1	7.7	7.6	7.5	8.4	8.5	6.9	7.2	9.2	8.1	8.1	7.2	7.0	7.4	8.4	8.8	8.6	8.6
Globocassidulina biora	100	16.7	23.5	18.2	33.3	57.9	36	83.3	42.9	22.2	40	66.7		22.2	22.2	36.4	33.3	50
G. crassa rossensis		66.7	70.6	72.7	66.7	36.8	64	16.7	42.9	77.8	56.7	33.3	100		77.8	63.6	66.7	50
Rosalina globularis		8.3																
Pullenia subcarinata		8.3				5.3			14.3		1.7			11.1				
Astrononion antarcticus			5.9											11.1				
Astrononion echolsi				9.1														
Miliammina arenacea											1.7			11.1				
Cassidulinoides parkerianus														33.3				
Cibicides refulgens														11.1				
Elphidium incertum																		
Nonionella bradii																		
Total specimen	1	12	17	11	12	19	25	6	7	9	60	15	2	9	9	22	6	2
Simple diversity	1.0	4.0	3.0	3.0	2.0	3.0	2.0	2.0	3.0	2.0	4.0	2.0	1.0	6.0	2.0	2.0	2.0	2.0
Abundance (/gram)	0.1	1.6	2.2	1.5	1.4	2.2	3.6	0.8	0.8	1.1	7.4	2.1	0.3	1.2	1.1	2.5	0.7	0.2
epifauna		8.3												11.1				
infauna	100	91.7	94.1	90.9	100	100	100	100	100	100	98.3	100	100	33.3	100	100	100	100
Agglutinated											1.7			11.1				
Porcelanous																		
hyline	100	100	100	100	100	100	100	100	100	100	98.3	100	100	88.9	100	100	100	100

Appendix 2-3. (continued)

depth (cm)	95	105	110	115	120	145	155	160	170	180	190	195	205	215	225	230	235
weight (gram)	9.1	8.0	10.7	13.0	11.1	10.0	9.8	12.9	16.5	19.2	20.1	12.3	13.0	10.8	9.7	18.3	21.8
Globocassidulina biora	39.6	60	83.1	50	92.3	83.3	38.5	60	100		60	71.4	50	66.7	25		33.3
G. crassa rossensis	58.5		15.5	50		16.7	46.2	40		100	40	28.6	50		75	100	66.7
Rosalina globularis																	
Pullenia subcarinata																	
Astrononion antarcticus																	
Astrononion echolsi																	
Miliammina arenacea			1.4											33.3			
Ca. parkerianus	1.9																
Cibicides refulgens							15.4										
Elphidium incertum					7.7												
Nonionella bradii		40															
Total specimen	53	5	71	4	13	6	13	10	4	1	5	7	2	3	4	2	3
Simple diversity	3.0	2.0	3.0	2.0	2.0	2.0	3.0	2.0	1.0	1.0	2.0	2.0	2.0	2.0	2.0	1.0	2.0
Abundance (/gram)	5.8	0.6	6.6	0.3	1.2	0.6	1.3	0.8	0.2	0.1	0.2	0.6	0.2	0.3	0.4	0.1	0.1
epifauna							15.4										
infauna	98.1	100	98.6	100	100	100	84.6	100	100	100	100	100	100	66.7	100	100	100
Agglutinated			1.4											33.3			
Porcelanous																	
hyline	100	100	98.6	100	100	100	100	100	100	100	100	100	100	66.7	100	100	100

Appendix 2-3. BF percentages (%), BF abundance, (BDI), fragmentation, yellow shell percentage, $CaCO_3$(%), TOC(%) and C/N ratio in core A10-01

depth (cm)	0	5	10	15	20	25	30	40	45	50	55	60	65	70	75	80	85	90
weight (gram)	7.1	7.7	7.6	7.5	8.4	8.5	6.9	7.2	9.2	8.1	8.1	7.2	7.0	7.4	8.4	8.8	8.6	8.6
Globocassidulina biora	100	16.7	23.5	18.2	33.3	57.9	36	83.3	42.9	22.2	40	66.7		22.2	22.2	36.4	33.3	50
G. crassa rossensis		66.7	70.6	72.7	66.7	36.8	64	16.7	42.9	77.8	56.7	33.3	100		77.8	63.6	66.7	50
Rosalina globularis		8.3																
Pullenia subcarinata		8.3				5.3			14.3		1.7			11.1				
Astrononion antarcticus			5.9											11.1				
Astrononion echolsi				9.1														
Miliammina arenacea											1.7			11.1				
Cassidulinoides parkerianus														33.3				
Cibicides refulgens														11.1				
Elphidium incertum																		
Nonionella bradii																		
Total specimen	1	12	17	11	12	19	25	6	7	9	60	15	2	9	9	22	6	2
Simple diversity	1.0	4.0	3.0	3.0	2.0	3.0	2.0	2.0	3.0	2.0	4.0	2.0	1.0	6.0	2.0	2.0	2.0	2.0
Abundance (/gram)	0.1	1.6	2.2	1.5	1.4	2.2	3.6	0.8	0.8	1.1	7.4	2.1	0.3	1.2	1.1	2.5	0.7	0.2
epifauna		8.3												11.1				
infauna	100	91.7	94.1	90.9	100	100	100	100	100	100	98.3	100	100	33.3	100	100	100	100
Agglutinated											1.7			11.1				
Porcelanous																		
hyline	100	100	100	100	100	100	100	100	100	100	98.3	100	100	88.9	100	100	100	100

Appendix 2-3. (continued)

depth (cm)	95	105	110	115	120	145	155	160	170	180	190	195	205	215	225	230	235
weight (gram)	9.1	8.0	10.7	13.0	11.1	10.0	9.8	12.9	16.5	19.2	20.1	12.3	13.0	10.8	9.7	18.3	21.8
Globocassidulina biora	39.6	60	83.1	50	92.3	83.3	38.5	60	100		60	71.4	50	66.7	25		33.3
G. crassa rossensis	58.5		15.5	50		16.7	46.2	40		100	40	28.6	50		75	100	66.7
Rosalina globularis																	
Pullenia subcarinata																	
Astrononion antarcticus																	
Astrononion echolsi																	
Miliammina arenacea			1.4											33.3			
Ca. parkerianus	1.9																
Cibicides refulgens							15.4										
Elphidium incertum					7.7												
Nonionella bradii		40															
Total specimen	53	5	71	4	13	6	13	10	4	1	5	7	2	3	4	2	3
Simple diversity	3.0	2.0	3.0	2.0	2.0	2.0	3.0	2.0	1.0	1.0	2.0	2.0	2.0	2.0	2.0	1.0	2.0
Abundance (/gram)	5.8	0.6	6.6	0.3	1.2	0.6	1.3	0.8	0.2	0.1	0.2	0.6	0.2	0.3	0.4	0.1	0.1
epifauna							15.4										
infauna	98.1	100	98.6	100	100	100	84.6	100	100	100	100	100	100	66.7	100	100	100
Agglutinated			1.4											33.3			
Porcelanous																	
hyline	100	100	98.6	100	100	100	100	100	100	100	100	100	100	66.7	100	100	100

Appendix 2-3. (continued)

depth (cm)	BDI	Fragmentation (%)	Yellow shell (%)	depth (cm)	gravel (%)	sand (%)	silt (%)	clay (%)	coarse (%)	TOC (%)	C/N	CaCO3 (%)
0			0	0	0	10.4	32.6	57.1	10.38	0.271	5.215	1.119
5	-0.8	30	20	5	0	8.8	34.0	57.2	8.75	0.237	5.543	1.401
10	-0.5	25	6.25	10	0	9.4	30.7	59.9	9.43	0.219	5.201	1.195
15	-1.0	50	20	15	0	10.3	30.7	59.0	10.3	0.193	5.393	1.174
20	-0.67	16.67	0	20	0	6.9	33.2	59.9	6.91	0.200	5.418	1.022
25	-0.83	38.89	5.56	25	4.09	15.4	28.4	52.1	19.45	0.228	5.167	1.370
30	-0.72	32	52	30	0	8.7	30.2	61.0	8.73	0.241	5.491	1.173
40	-0.83	33.33	16.67	35	0	6.6	31.3	62.1	6.63	0.237	5.373	1.163
45	-0.83	16.67	33.33	40	0	8.9	32.0	59.1	8.89	0.230	5.481	1.148
50	-1	100	11.11	45	0	9.4	34.2	56.4	9.44	0.222	5.210	1.150
55	-0.93	27.59	8.62	50	0	11.8	31.5	56.7	11.82	0.242	5.290	1.093
60	-1	53.33	0	55	0	9.8	31.7	58.5	9.83	0.244	5.591	1.124
65	-1	0	0	60	2.99	16.3	27.3	53.4	19.28	0.265	5.348	1.260
70	0.5	0	0	65	0	14.8	28.1	57.1	14.76	0.249	5.809	0.965
75	-0.89	44.44	0	70	2.38	16.3	27.4	54.0	18.69	0.239	5.349	1.120
80	-0.95	45.45	22.73	75	0	16.1	30.8	53.0	16.12	0.238	5.366	1.104
85	-0.67	33.33	33.33	80	0	16.1	30.3	53.7	16.06	0.209	5.320	0.966
90	-1	0	0	85	0	14.2	31.2	54.5	14.23	0.159	3.896	1.423
95	-0.92	32.69	36.54	87.5						0.273	5.405	1.541
100	-1	100	0	90	0	13.1	32.4	54.5	13.11	0.188	5.437	0.901
105	-0.67	0	33.33	95	3.66	11.9	32.1	52.3	15.59	0.138	5.425	0.777
110	-0.42	8.70	21.43	100	0	14.4	32.9	52.8	14.37	0.137	5.462	0.843
115	-0.5	25	25	105	0	15.1	31.7	53.2	15.11	0.136	5.176	0.946
120	-0.42	25	8.33	110	0	18.1	33.9	48.1	18.06	0.088	5.732	1.168

Appendix 2-3. (continued)

depth (cm)	BDI	Fragmentation (%)	Yellow shell (%)	depth (cm)	gravel (%)	sand (%)	silt (%)	clay (%)	coarse (%)	TOC (%)	C/N	CaCO3 (%)
145	-0.83	0	40	115	15.43	30.6	23.4	30.6	46.01	0.082	5.441	1.546
155	-0.27	9 09	27 27	120	0.59	23.1	33.0	43.3	23.69	0.093	5.370	1.402
160	0.3	30	11	125	0.55	21.4	55.5	22.6	21.94	0.086	5.121	1.312
170	-0.5	50	50	130	0	17.4	35.1	47.6	17.35	0.091	5.538	1.387
180	0	0	0	135	2.3	21.3	51.6	24.8	23.63	0.072	4.643	1.454
190	1	40	60	140	12.62	21.8	41.6	24.0	34.44	0.084	5.158	1.524
195	-0.57	42.86	14.29	145	6.88	24.9	28.6	39.6	31.82	0.088	5.559	1.274
205	-0.5	100	0	150	2.72	14.0	56.3	27.0	16.69	0.102	5.553	1.562
215	-1	0	0	155	12.41	24.2	25.8	37.6	36.57	0.040	5.409	2.554
225	0	50	0	160	9.64	25.5	25.7	39.2	35.09	0.047	5.484	2.462
230	0	50	0	165	0.58	15.7	44.6	39.2	16.28	0.103	6.109	1.299
235	0.33	33.3	0	170	10.82	28.9	22.4	37.9	39.74	0.065	8.461	1 215
				175	49.62	36 9	5 0	8.4	86.56	0.022	9 430	1.449
				180	22.03	43.7	13.3	21.0	65.72	0.021	8.951	1.303
				185	18.24	34.8	18.6	28.4	53.03	0.027	5.142	1.165
				190	15.29	41.1	13.1	30.5	56.43	0.045	6.149	1.658
				195	12.89	35.9	20.1	31.2	48.74	0.048	5.482	1.775
				200	9.08	24.9	28.4	37.6	34	0.082	5 211	1.622
				205	12.79	34.0	13.8	39.4	46.82	0.100	5.467	1.942
				210	8.23	23.6	31 7	36.5	31.82	0.066	5.191	1.411
				215	10.07	23.6	26.4	39.9	33.63	0.050	5.603	2.139
				220	20.56	34.0	17.8	27.6	54.59	0.042	5.308	2.422
				225	7.13	38.6	21.7	32.5	45.77	0.043	5.345	2.375
				230	16.33	36.3	21.0	26.5	52.58	0.043	6.827	2.270
				235	17.85	36.4	20.4	25.4	54.29	0.047	7.645	2 276

Appendix 2-4. BF percentages (%), BF abundance, (BDI), fragmentation, yellow shell percentage, $CaCO_3$(%), TOC(%) and C/N ratio in core A10-02

depth (cm)	0	5	10	15	20	25	30	35	40	45	50	60
weight (gram)	9.3	10.5	9.1	9.3	10.8	12.2	9.2	10.1	11.1	9.3	7.6	11.5
Globocassidulina biora	20	9.1		22.9	20.9	25	11.1		35			23.8
G. crassa rossensis	20	38.6		17.1	11.6	25	11.1		15			19
Rosalina globularis	2.5											
Pullenia subcarinata	7.5	13.6			2.3				20			28.6
Astrononion echolsi	7.5	13.6		5.7	4.7							
Astrononion antarcticus					2.3							
Miliammina arenacea	15	13.6		34.3	30.2	25	55.6	80	5	100	42.9	4.8
Cassidulinoides parkerianus	27.5	11.4	100	17.1	23.3		22.2		10		57.1	9.5
Cassidulinoides porrecta												
Cibicides refulgens				2.9								4.8
Trifarina angulosa					4.7	25		20				
Nonionella bradii												4.8
Lingulina translucida												4.8
Elphidium incertum												
Elphidium sp1												
Quinqueloculata seminula												
Pyrgo pentagonica												
Neogloboquadrina pachyderma L												
Glibigerinita glutinata												
epifauna	17.5	13.6		37.1	30.2	25	55.6	80	5	100	42.9	9.5
infauna	47.5	61.4		40	39.5	75	22.2	20	70		0.0	76.2
Agglutinated	15	13.6		34.3	30.2	25	55.6	80	5	100	42.9	4.8
Porcelaneous												
Hyaline	85	86.4	100	65.7	69.8	75	44.4	20	95		57.1	95.2
BF simple diversity	7	6	1	6	8	4	4	2	6	1	2	8
Abundance (number per gram)	4.3	4.2	0.2	3.8	4.0	0.3	1.0	0.5	1.8	0.3	0.9	1.8
specimens counted	40	44	2	35	43	4	9	5	20	3	7	21

Appendix 2-4. (continued)

depth (cm)	65	70	75	80	90	95	100	105	110	115	120	125
weight (gram)	11.7	9.7	9.1	11.6	11.4	13.0	10.3	13.7	13.6	10.4	14.1	18.1
Globocassidulina biora		27.3	18.8			21.4	20.8	17.7	17.2	33.3	33.3	100
G. crassa rossensis		9.1			14.3	21.4	4.2	11.5	17.2	36.5	31	
Rosalina globularis												
Pullenia subcarinata		27.3	18.8		7.1	14.3				1.6		
Astrononion echolsi												
Astrononion antarcticus						7.1				1.6		
Miliammina arenacea	100	36.4	31.3	100	57.1	28.6	62.5	69	44.8	12.7	1.2	
Cassidulinoides parkerianus			25.0		14.3		8.3	0.9	20.7	9.5	32.1	
Cassidulinoides porrecta										1.6		
Cibicides refulgens			6.3			7.1	4.2	0.9				
Trfarina angulosa					7.1							
Nonionella bradii												
Lingulina translucida												
Elphidium incertum												
Elphidium sp1											1.2	
Quinqueloculata seminula												
Pyrgo pentagonica											1.2	
Neogloboquadrina pachyderma L										1.6		
Glibigerinita glutinata										1.6		
epifauna	100	36.4	37.5	100	57.1	35.7	66.7	69.9	44.8	12.7	2.4	
infauna		63.6	37.5		28.6	57.1	25	29.2	34.5	71.4	65.5	100
Agglutinated	100	36.4	31.3	100	57.1	28.6	62.5	69	44.8	12.7	1.2	
Porcelaneous											1.2	
Hyaline		63.6	68.8		42.9	71.4	37.5	31	55.2	87.3	97.6	100
BF simple diversity	1.0	4.0	5.0	1.0	5	6	5	5	4	9	6	1
Abundance (number per gram)	0.3	1.1	1.8	0.2	1.2	1.1	2.3	8.2	2.1	6.1	6.0	0.1
specimens counted	4.0	11.0	16.0	2.0	14	14	24	113	29	63	84	2

Appendix 2-4. (continued)

depth (cm)	130	137	155	160	165	170	175	180	189	195	200	205
weight (gram)	12.2	24.4	18.4	20.6	20.6	22.3	21.1	19.4	20.3	19.2	19.7	17
Globocassidulina biora	42.9	68.8	33.3	55.3		12	33.6	17.6	70.2		65.7	10
G. crassa rossensis		31.3	33.3	42			35.5	17.6	20.2		33.3	
Rosalina globularis												
Pullenia subcarinata												
Astrononion echolsi												
Astrononion antarcticus												
Miliammina arenacea	57.1		33.3	2.67	100	88	11.2	64.7	9.2	100	0.5	90
Cassidulinoides parkerianus							18.7		0.4		0.5	
Cassidulinoides porrecta												
Cibicides refulgens												
Trifarina angulosa												
Nonionella bradii												
Lingulina translucida												
Elphidium incertum												
Elphidium sp1.												
Quinqueloculata seminula												
Pyrgo pentagonica							0.93					
Neogloboquadrina pachyderma L												
Glibigerinita glutinata												
epifauna	57.1		33.3	2.67	100	88	12.1	64.7	9.2	100	0.5	90
infauna	42.9	100	66.7	97.3		12	69.2	35.3	90.4		99.0	10
Agglutinated	57.1		33.3	2.67	100	88	11.2	64.7	9.2	100	0.5	90
Porcelaneous							0.93					
Hyaline	42.9	100	66.7	97.3		12	87.9	35.3	90.8		99.5	10
BF simple diversity	2	2	3	3	1	2	5	3	4	1	4	2
Abundance (number per gram)	0.57	0.66	0.33	7.28	0.24	1.12	5.08	0.88	13.4	0.7	10.3	0.6
specimens counted	7	16	6	150	5	25	107	17	272	13	204	10

Appendix 2-4. (continued)

depth (cm)	210	215	220	225	230	235	240	245	250	255	260	265	270
weight (gram)	14 1	18 7	19 5	15.2	15	13 8	18.2	23	18 7	16 5	19 5	18 1	15 8
Globocassidulina biora	62 2	72 6	45 8	21 2	45 2	40 9	60 2	68 5	39 2	52 6	59 2	26 5	26 7
G crassa rossensis	24 4	12 2	46.5	24.2	38 7	42 4	35.2	29 5	47 4	40 8	36 2	33 8	57 8
Rosalina globularis										0 51			
Pullenia subcarinata					1 29								
Astrononion echolsi													
Astrononion antarcticus			0 17										
Miliammina arenacea	4 2	5 49	5 98	3 03	12 9	9 09	0 38	0 79	13.4	1 53	2 63	29 4	2 22
Cassidulinoides parkerianus	8.4	7 59	1 37	30.3		4 55	1 89	1 18		4 08	1 97	10 3	13 3
Cassidulinoides porrecta													
Cibicides refulgens	0 84			18 2	0 65								
Trifarina angulosa					0 65								
Nonionella bradii													
Lingulina translucida													
Elphidium incertum						1 52							
Elphidium sp1		2 11			0 65	1 52	2.27			0 51			
Quinqueloculata seminula			0 17										
Pyrgo pentagonica													
Neogloboquadrina pachyderma L				3 03									
Glibigerinita glutinata													
epifauna	5 04	5 49	6 15	21 2	13 5	9 09	0 38	0 79	13 4	2 04	2 63	29 4	2 22
infauna	86 6	86 9	92 3	45 5	86 5	86 4	97 7	98	86 6	93 9	95 4	60 3	84 4
Agglutinated	4 2	5 49	5 98	3 03	12 9	9 09	0.38	0.79	13 4	1 53	2 63	29 4	2 22
Porcelaneous			0 17										
Hyaline	95 8	94 5	93.8	97	87 1	90.9	99.6	99.2	86 6	98.5	97 4	70 6	97 8
BF simple diversity	5	5	6	6	7	6	5	4	3	5	4	4	4
Abundance (number per gram)	8 46	12 7	29 9	2 18	10 4	4 8	14 5	22 1	5 19	11 9	7 8	3 77	2 84
specimens counted	119	237	585	33	155	66	264	508	97	196	152	68	45

Appendix 2-4. (continued)

Depth (cm)	BDI	fragmentation (%)	Yellow shell (%)	gravel (%)	sand (%)	silt (%)	clay (%)	coarse (%)	TOC (%)	C/N	CaCO3 (%)
0	-0.31	50	12.5	0	3.48	27.46	69.06	3.48	0.484	5.413	1.736
5	-0.86	9.5	0	0.23	3.48	29.46	66.83	3.71	0.417	5.404	1.892
10				0	1.6	31.21	67.19	1.6	0.380	5.233	1.697
15	-0.71	28.6	0	0.28	5.98	35.06	58.68	6.26	0.390	5.436	1.685
20	-0.50	35.7	0	0	6.75	33.55	59.7	6.75	0.392	5.382	1.616
25	-1.00	50	0	23.64	4.61	25.98	45.77	28.25	0.419	5.394	1.499
30	-1.00	100	0	1.88	6.19	33.95	57.98	8.07	0.433	5.389	1.510
35	-1.00	100	0	0	4.83	32.38	62.79	4.83	0.379	5.187	1.531
40	-0.90	20	0	0	4.03	36.36	59.61	4.03	0.342	5.150	1.600
45	-1.00	100	0	0	2.81	32.2	64.99	2.81	0.350	4.977	1.989
50				0	3.26	34.38	62.36	3.26	0.374	5.357	1.501
55				0	4.97	31.06	63.97	4.97	0.349	5.348	1.241
60	-1.00	22.2	0	0	4.51	36.99	58.5	4.51	0.345	5.324	1.369
65				0	3.46	37.5	59.04	3.46	0.376	5.264	1.516
70	-1.00	50	0	3.51	3.25	33.87	59.37	6.76	0.337	5.238	1.350
75	-1.00	33.3	0	0	4.89	35.97	59.14	4.89	0.322	5.302	1.601
80				0	7.07	38	54.93	7.07	0.315	5.316	1.540
85				0	7.07	38	54.93	7.07	0.284	5.107	1.452
90	-1.00	50	0	0	4.87	33.48	61.65	4.87	0.261	5.307	1.362
95	-0.50	50	0	6.73	5.78	32.43	55.06	12.51	0.281	5.328	1.458
100	-1.00	83.3	0	0	4.92	35.23	59.85	4.92	0.301	5.273	1.472
105	-0.97	30.3	0	1	7.11	31.24	60.65	8.11	0.304	5.247	1.442
110	-0.80	20	10	6.78	9.86	29.94	53.42	16.64	0.247	5.066	1.863
115	-0.64	36.4	4.5	0.28	10.04	31.34	58.34	10.32	0.234	5.290	1.689
120	-0.76	24.1	5.6	2.45	24.19	26.83	46.54	26.64	0.127	5.291	1.607
125	-0.50	100	0	0.41	35.36	27.86	36.37	35.77	0.063	5.849	2.000
130	-0.33	66.7	33.3	1.08	26.8	34.81	37.31	27.88	0.071	6.264	2.307
135				0	40.82	26.16	33.01	40.82	0.060	7.448	2.458
137	-0.88	25	37.5	0	29.49	45.96	24.56	29.49	0.052	18.092	2.557

Appendix 2-4. (continued)

Depth (cm)	BDI	fragmentation (%)	Yellow shell (%)	gravel (%)	sand (%)	silt (%)	clay (%)	coarse (%)	TOC (%)	C/N	CaCO3 (%)
145				0	52.76	33.96	13.28	52.76	0.048	159.297	2.545
150				0	33.4	30.33	36.27	33.4	0.063	35.027	2.490
155	-1.00	100	50	0	34.51	36.05	29.44	34.51	0.059	23.442	2.392
160	-0.99	36.1	38.8	0	34.51	36.05	29.44	34.51	0.126	10.548	2.366
165				0	28.82	29.48	41.71	28.82	0.065	11.431	2.260
170	-0.67	100	66.7	0	41	26.31	32.7	41	0.069	8.472	2.219
175	-0.59	34.1	36.4	0.11	25.96	14.18	59.75	26.07	0.119	11.053	1.757
180	-1.00	16.7	66.7	0.23	36.49	33.46	29.82	36.72	0.049	4.526	2.520
185				0.23	36.49	33.46	29.82	36.72	0.083	12.528	2.063
189	-0.89	32.9	32.1						0.090	47.141	2.132
190				0.37	33.67	29.06	36.91	34.04	0.064	22.792	2.127
195	-1.00	0	0	0.23	34.71	27.41	37.65	34.94	0.085	94.979	2.136
200	-0.96	35.6	27.2	0	43.73	24.58	31.7	43.73	0.060	18.051	2.249
205	-1.00	100	0	0	25.45	37.54	37.02	25.45	0.122	13.807	1.830
210	-0.65	32	35	0.28	17.24	21.76	60.72	17.52	0.184	7.313	1.624
215	-0.55	12.9	15.1	1.48	25.67	30.88	41.97	27.15	0.132	5.957	1.859
220	-0.94	12.0	19.3	0.31	35.07	19.58	45.05	35.38	0.150	10.857	1.265
225	-0.20	6.7	13.3	0	13.5	39.35	47.14	13.5	0.151	7.002	2.036
230	-0.63	13.8	4.6	0	9.87	39.3	50.83	9.87	0.228	5.147	2.467
235	-0.55	29.1	5.5	0.76	10.07	35.51	53.66	10.83	0.214	5.073	1.657
240	-0.32	11.9	2.4	0.73	21.62	38.09	39.56	22.35	0.085	5.865	1.819
245	-0.89	6.4	5.4	3.13	19.31	43.63	33.93	22.44	0.120	8.789	1.506
250	-0.98	34.5	54.8	0.82	20.03	43.61	35.54	20.85	0.086	5.130	2.072
255	-0.64	16.4	12	0.95	19.06	39.77	40.22	20.01	0.108	7.168	2.140
260	-0.10	6.9	15.9	0.18	25.83	37.7	36.3	26.01	0.113	10.437	1.944
265	-0.85	14.6	9.8	0	25.89	35.98	38.13	25.89	0.128	8.389	1.825
270	0.11	7.9	23.7	0.68	14.47	32.23	52.63	15.15	0.163	7.256	1.872

Appendix 4-1. Benthic foraminifera (larger than 63um) percentages in core 97-02

species \ depth(cm)	0	10	20	30	40	50	60	70	80	90	100	110	120	130	140	150	160	170	180	190
Gaudryina haeringensis					0.2			0.4		0.3	0.2	0.2	1.2	0.5			0.5			
Proteonia spp.		0.2	0.1																	
Textularia spp.		1.2	0.4	1.8	1.4	2.1	2.1	1.2	2.0	2.4	1.9	1.8	2.6	3.4	2.5	3.7	1.6	1.9	1.0	6.2
Tritaxia donghaiensis			0.1							0.2	0.3									
Verneuilina sp.			0.7	1.1	0.8	0.1		0.2	0.6		1.1	0.6	0.2			0.5				
Ammomassilina spp.	0.3	1.0	2.0	0.9	0.4	0.1	0.3	0.2		0.3	0.2		0.2		0.3					
Edentostomina cultrata					0.1															
Miliammina spp.	0.3	0.3	0.1	0.1	1.2	0.9	0.3	1.2	2.0	0.7	0.8	1.4	0.5	1.2	1.1	2.3	0.9	0.7	0.3	0.7
Pyrgo elongata													0.5		0.3					
Quinquelocolina contorta												0.6				1.4		0.5	0.7	0.9
Quinqueloculina lamarckiana																0.5				
Quinqueloculina rotunda												0.4		1.2	0.5		0.2			2.0
Quinqueloculina sabulosa	0.6	0.5	1.2	0.7	1.0	0.4	1.6	0.7	1.8	1.0	0.6	1.6	3.1	2.9	4.4	1.9	2.7	0.5		1.3
Quinqueloculina seminula								0.2				0.4			0.5		0.2			
Quinqueloculina seminulangula					0.1		0.2	0.3			0.5	0.6	1.2	1.5	1.4			0.2	2.1	
Quinqueloculina tikutoensis																	0.2		0.3	
Quinqueloculina vulgaris												0.2	0.2	1.2	1.1	1.9	1.3	9.3	5.1	2.9
Quinqueloculina spp.							0.2						0.2	0.2						
Sigmoilina tenuis		0.5	0.4	0.2	0.4	0.4		0.1		0.3	0.3	0.4			0.3	0.5	0.2	0.2		0.2
Sigmoilina spp.																	0.4			
Sigmoilopsis asperula	0.6	0.7	1.1	0.8	0.3	1.3	1.4	1.2	2.0	2.1	2.4	2.6	1.7	2.4	1.6	0.5	2.2	1.7	1.0	2.4
Spiroloculata communis		0.2								0.3			0.2	0.2						0.4
Spiroloculina laevigata																	0.4		0.3	
Triloculina tricarinata																				
Triloculina trigonula					0.2		0.5	0.1	0.1			0.2	0.2				0.2			
Triloculina spp.																	0.2			
Amphicoryna sublineata		0.2					0.2										0.2			
Amphicoryna sp.																		0.2		
Botuloides sp.																	0.2			
Dentalina cf. *basiplanata*				0.2					0.1											
Dentalina communis				0.1						0.2										
Dentalina decepta														0.2						

Appendix 4-1. (continued)

species \ depth(cm)	0	10	20	30	40	50	60	70	80	90	100	110	120	130	140	150	160	170	180	190
Dentalina extensa										0.2										
Dentalina sp.																				0 2
Esosyrinx sp.																				0.2
Fissurina spp.	1.2	1 0	1 1	0 4	0.5	0.6	0.7	0 6	0.7	0.9	0.8	0.4	1 0	2.2	1 1	0 5	0 9	0 7	2 1	2.0
Lagena spp.	0.6		0.1		0 1	0.4		0.2		0.5	0.3	0.6	0 7	1.2	0.5	0.9		0.2		0.9
Lenticulina calcar										0 2	0 5	0 4				0.5	0.2			
Lenticulina costata											0 2									
Lenticulina iotus		0 5	0 1	0 4	0 2	0 1	0.7	0 2	0.1	0.3	0.6	0.2		0.2	0.5		0 4	0 5		
Lenticulina tumida														0 2	0.3					
Lenticulina sp.		0.2	0.3		0.4	0.3	0 3	0.3	0.3	0 2	0 3	0 4	0 2	0 2				0 5		
Polymorphina sp.																				
Saracenaria italica		0 2									0.2									
Sigmomorphina sp																				
Bifarina sp.																				0.2
Bolivina robusta	22.7	27.6	30.9	33.0	32 5	29 8	36.1	33.1	35.7	34.5	34.4	23 6	19 7	21.3	15 0	20.8	24.3	22.6	19 2	10 0
Brizalina seminuda	3.4	1.3	1.1	0 5	0 2	1.2	0.5	1.1	0 7	0.3	1.3	0 8	1 7	1 0	1 1	0 5	0.4	0.7	0.7	0.2
Brizalina striatula	0.3								0.1	0.2	0.2	0 4	0 2	1.2	0.3	0 5	0 7	0 2	0 7	
Brizalina spp.				0.1	0.2	0.9	0 3	0 1	0 7	0 2		0.4	1 0	0.7			0.9			0.2
Bulimina marginata	7 2	5.3	6.7	5.1	6.5	7 4	5.0	5 8	6.2	5.3	3.3	3.4	4 8	2 2	3 6	1 9	2.7	4.0	2.7	0.7
Cassidulina carinata	7.8	4 8	4 1	4 5	4 8	3.6	5.4	3.8	0.8	2.6	1.3	1.6	4 6	1.5	3.8	0 9	1.8	1 7	0 7	1 3
Fursenkoina pauciloculata												0 6		0.2	0 3					
Fursenkoina schreibersiana				0.1	0.1	0.1	0.2	0.1	0.3		0.2						0 2	0 2		
Globobulimina notovata		0.2														0.5		0 2		
Globocassidulina subglobosa	1 2	1 7	0.3	0.7	0.9	0.7	0.5	1.0	0.6	0 9	0.5	1 2	1 2	1.5	0.8	1.4	1.3			1.3
Guembelitria vivans			0.1	0 2		0.4	0.2		0.7						1.1					
Hopkinsina pacifica	0.3	0 2		0 4					0.1	0 5			0.2		0 3	0.5	0 2		0 3	0.2
Islandiella islandica																	0.4	0.5	2 4	4.6
Rectobolivina bifrons striatula																				
Siphouvigerina porrecta	0 3																			
Stainforthia complanata	0 3	0 2	0 3	0 7	0.1			0.2									0 2			
Trifarina angulosa			0 3	0 4	0 2	0 7		0 2		0.5		0.2	0 2	0.2	0.3	0 9			0 3	0 4
Trifarina bradyi						0 1														
Uvigerina canariensis	2.5	4.0	3.4	2.5	2.6	3.0	2.9	2 5	2.1	1.9	2 7	1.4	1.7	1.2	1.9	2 8	2 2	2 6	1 0	0.4

Appendix 4-1. (continued)

species \ depth(cm)	0	10	20	30	40	50	60	70	80	90	100	110	120	130	140	150	160	170	180	190
Uvigerina dirupta														0.2						
Virgulopsis orientalis	0.3	0.3	0.4	0.1	0.3	0.3	0.3	0.7	0.4	0.7	0.5	0.4	1.9	0.2	1.1		0.4	0.2	0.3	0.4
Astrononion tasmanensis	2.8	3.7	2.6	4.3	4.2	2.1	3.8	3.8	3.8	3.1	4.6	3.0	1.2	3.6	4.6	2.3	4.0	1.7	3.1	1.5
Cribrononion incertum																				
Cribrononion porisuturalis																				
Cribrononion subincertum						0.1												0.2	0.3	0.2
Cribrononion sp.																				
Elphidiella Kiangsuensis																				
Elphidium advenum	1.2	1.3	2.7	2.2	2.1	3.0	3.8	3.0	3.5	2.2	4.9	3.0	5.3	4.1	4.6	4.2	3.8	4.8	5.8	4.9
Elphidium crispum																				
Elphidium magellanicum																3.2	4.2	8.6	15.4	6.0
Florilus decorus	1.6	0.5	1.4	1.3	0.4	1.3	1.6	0.8	1.3	2.2	1.0	1.2	2.2	3.6	2.2	9.7	2.2	1.0	1.0	3.3
Melonis sp.																				
Nonion akitaense														1.7		0.5		1.0		
Nonion stella																				
Nonion sp.																				
Nonionella jacksonensis	2.2	0.3	1.6	0.6	0.5	0.7		0.2	0.6	0.9	0.2	0.2		1.0	0.8		0.4	1.4		0.9
Nonionella magnalingua	0.3	0.5		0.1	0.1												0.2			
Nonionella sp.	1.9	1.2	0.1	0.7	0.3			0.2	0.6	0.5	0.2	1.2		1.9						1.3
Protelphidium compressum																		0.2	0.7	0.7
Pseudononionella sp.																				
Pullenia bulloides																				
Pullenia quinqueloba	0.3	0.2	0.5	0.1	0.1	0.1		0.2	0.6		0.3	0.4	0.2		0.5	0.9				1.1
Spirillina sp.			0.1																	
Stomoloculina multangula																				
Ammonia annectens																				
Ammonia compressiuscula			1.5	0.8	2.2	1.3	4.8	1.8	2.1	2.7	4.9	5.1	2.9	3.4	1.9	1.9	2.5	2.6	2.1	2.2
Ammonia confertitesta																				
Ammonia convexdorsa																	0.7	1.2		1.8
Ammonia ketienziensis angul.	5.3	12.0	6.3	7.6	9.1	8.2	5.0	6.3	3.9	5.8	7.0	6.9	5.5	6.8	7.7	5.1	5.4	4.0	2.7	2.7
Ammonia limbatobeccarii	0.3		0.3	0.1			0.7	0.4	0.3		0.2	0.2	0.5				0.5	0.2	1.0	1.3

Appendix 4-1. (continued)

species \ depth(cm)	0	10	20	30	40	50	60	70	80	90	100	110	120	130	140	150	160	170	180	190
Ammonia multicella																		0.2		
Ammonia pauciloculata	18.1	13.3	11.6	14.4	15.0	14.4	9.3	15.8	11.0	9.8	7.8	10.1	6.0	7.0	9.8	5.1	13.9	10.2	8.6	3.8
Ammonia tepida																		0.2	2.7	1.3
Buccella frigida																		0.2	1.4	0.7
Cancris auriculus	0.3				0.5	1.0	0.2	0.3	0.7	0.2		0.2	1.2	1.2			0.5	0.2	0.3	0.9
Cibicides lobatulus	0.3	0.2		0.2			0.2					0.4	0.5	0.2	0.5		0.2	0.7	1.0	0.2
Cibicides pseudoungerianus	1.2	0.2	0.4	0.6	0.7	0.4	0.5	0.6	0.7	0.5	0.8	1.2	1.9	1.2	0.5	0.9	0.7	1.4	1.0	2.7
Cibicides sp.								0.2				0.2	0.2		0.3	0.5	0.2	0.2	0.7	0.9
Cibicidina sp.																				
Discorbinella bertheloti																				
Epistominella naraensis	6.9	4.2	2.5	1.9	2.2	2.4	0.7	1.8	2.0	2.7	1.1	2.6	6.0	3.4	4.4	4.6	3.4	1.0	3.1	7.7
Eponides repandus						0.3							0.2				0.2			
Eponides sp.																				
Gavelinopsis sp.	1.6	3.7	3.7	0.8	0.9	1.9	1.6	2.8	2.8	2.7	2.5	3.8	5.0	1.9	2.5	4.6	2.7	1.0	1.0	1.5
Geminospira simaensis																				0.2
Gyroidina nipponica	2.2	3.0	5.3	3.1	2.2	2.4	2.6	2.8	1.4	1.4	0.3	1.0	0.2	0.2	0.8	0.5	1.1	1.4	1.0	0.4
Gyroidina sp.																			0.3	
Hanzawaia nipponica	0.9	1.0	0.3	1.2	0.7	0.4	1.2	0.4	0.4	1.0	2.1	1.8	3.1	3.1	3.3	3.2	0.5	1.0		4.2
Heterolepa dutemplei	0.3	0.2	0.8	0.7	0.9	1.0	1.9	0.9	2.0	1.4	2.7	3.4	1.7	1.5	3.3	0.5	0.5	0.7		
Hyalinea balthica	0.6	1.0	0.7	1.7	1.3	1.3	0.9	0.6	3.1	2.2	2.1	2.6	2.2	1.0	1.6	1.4	0.9	0.7	0.7	
Hyalinea sp.	0.9	1.3	1.4	1.7	0.4	1.3	0.5	1.5	0.7	0.5	0.5	0.8	1.2	0.5	0.5	1.9	0.2	1.0	0.3	1.5
Lamarkina scabra																				0.2
Neoeponides procera																				
Pararotalia nipponica															0.3	1.9	1.1	1.7	3.4	1.1
Psendoeponides japonica	0.3	0.5	0.5	0.2	0.4	0.3	0.2	0.1	0.6	0.9	0.3	1.2	0.2		1.1	0.9	0.5	0.2	0.3	0.7
Pseudogyroidina sinensis											0.8	1.4	0.7	0.7	1.1	0.9	0.2			
Pseudorotalia indopacifica										0.2	0.3	0.2								
Pulsiphonina sp.	0.3			0.1	0.2	0.4	0.3	0.2	0.1	0.5	0.2	0.2	0.2		0.3		0.2			
Rosalina bradyi				0.1								0.2								1.8
Rosalina australis				0.1	0.3		0.3	0.1		0.5				0.7	0.8		0.5	1.0	0.3	1.5
Rotalia sp.																				
Sphaeroidina bulloides				0.1										0.2	0.3					
Seabrookea sp.				0.1						0.2				0.2	0.3					0.2
counting BF	321	602	734	845	1114	674	579	1294	715	582	630	495	416	413	366	216	552	421	292	452

Appendix 4-1. (continued)

species \ depth(cm)	200	210	220	230	240	250	260	270	280	300	320	340	360	380	400	420	460	480	510
Gaudryina haeringensis										0.2	0.4	0.3				0.6			0.9
Proteonia spp.																			
Textularia spp.	2.2	1.3	1.1	0.4	1.3	0.4	0.2	1.0	1.3	0.5	0.4	0.6	0.9			0.9	1.3		0.9
Tritaxia donghaiensis				0.4															
Verneuilina sp.	0.4			0.8		0.8	0.2		0.1										
Ammomassilina spp.																			
Edentostomina cultrata	0.2			0.4															
Miliammina spp.	0.4	0.4	0.4	0.4	0.3	0.4	0.2			0.2				0.2				0.5	
Pyrgo elongata				0.4														0.5	
Quinquelocolina contorta		0.7				0.4		0.3	0.3	0.2	0.4		0.4						
Quinqueloculina lamarckiana	0.4										0.4								0.9
Quinqueloculina rotunda	0.7	0.7			1.3		0.2	1.3	2.1	2.7	2.6	1.0	0.4		0.5			0.5	
Quinqueloculina sabulosa	1.3	0.4	0.8	0.4				0.3	0.3	0.2									
Quinqueloculina seminula						0.4							0.2						
Quinqueloculina seminulangula	0.4		0.4		0.3	0.4		1.0		0.2								0.5	
Quinqueloculina tikutoensis							0.4		0.3										
Quinqueloculina vulgaris	2.8	13.4	2.3	7.5	8.6	2.7	1.1	1.3	1.1	1.2	2.1	0.3	1.8	0.9	2.1	0.6	3.3	5.2	5.2
Quinqueloculina spp.		2.7	1.5	1.1	0.6		1.5	1.0		0.7		3.5	1.5	1.6	1.6	0.6	1.3	1.9	1.7
Sigmoilina tenuis		0.7	0.4																
Sigmoilina spp.	0.9	0.7	0.4			1.5	0.9	0.3		2.4	1.7	0.6	1.3	0.2	1.4	1.2	1.7	1.4	0.9
Sigmoilopsis asperula	0.7	0.4	0.8	0.8		0.8	0.4	1.0	0.7	0.2									
Spiroloculata communis						1.5	0.4		0.1										
Spiroloculina laevigata	0.2							0.3			0.4								
Triloculina tricarinata	0.2																		
Triloculina trigonula					0.3									0.2			0.4		
Triloculina spp.																			
Amphicoryna sublineata	0.2													0.2					
Amphicoryna sp.																			
Botuloides sp.																			
Dentalina cf. *basiplanata*																			
Dentalina communis																			
Dentalina decepta																			

Appendix 4-1. (continued)

species \ depth(cm)	200	210	220	230	240	250	260	270	280	300	320	340	360	380	400	420	460	480	510
Dentalina extensa																			
Dentalina sp																			
Esosyrinx sp.	0.2																		
Fissurina spp.	2.2	1.3	3.0	2.6	2.9	2.3	1.3	2.0	1.1	1.0		1.9	1.1	2.3	1.2	2.1	1.7	0.9	0.9
Lagena spp.	0.4			0.8	0.3							0.3	0.4	0.2		0.3		0.5	
Lenticulina calcar		0.2												0.2					
Lenticulina costata																			
Lenticulina iotus			0.4	0.4	0.3			0.7	0.3	0.2									
Lenticulina tumida																			
Lenticulina sp.	0.4				1.0			0.3											0.9
Polymorphina sp.														0.2					
Saracenaria italica	0.2																		
Sigmomorphina sp.					0.3		0.2					0.3							
Bifarina sp.																			
Bolivina robusta	21.8	5.1	12.4	11.3	11.1	11.7	9.6	10.3	16.7	5.4	2.1	1.9	0.2			0.3	4.6	0.9	0.9
Brizalina seminuda	0.4	0.7	0.4			0.4			0.6	0.2	0.4		0.2		0.2				
Brizalina striatula	0.0	0.4	2.3	0.8	1.0		1.3	1.0	0.6	2.2	1.3	1.0	1.3	1.6	0.2	1.5	0.8	0.9	
Brizalina spp.	0.4	0.7	0.8		0.6	0.4	0.2	0.3	1.1	0.2			1.1	0.7	0.2	0.3		0.5	0.9
Bulimina marginata	2.6	1.6	0.8	1.1	3.2	2.3	2.6	1.7	2.9	2.0	0.9	0.3	0.4	0.2			0.8	1.4	0.9
Cassidulina carinata	1.1	0.2	1.9	0.8	0.6		0.9	0.3	2.4	0.5							0.4	0.5	
Fursenkoina pauciloculata					0.3				0.3										
Fursenkoina schreibersiana			0.4																
Globobulimina notovata	0.2			0.4															0.9
Globocassidulina subglobosa	0.7			0.8	1.3	1.1	0.4	0.7	1.1	1.2		1.0	1.1	1.8	0.9	0.9	0.4	0.9	1.7
Guembelitria vivans	0.2				0.3		0.2												
Hopkinsina pacifica			0.4																
Islandiella islandica	0.4	0.4	0.4		0.3	0.4		0.7	0.1	1.0		1.0	0.9			0.3		0.9	0.9
Rectobolivina bifrons striatula																		0.5	
Siphouvigerina porrecta																			
Stainforthia complanata																			
Trifarina angulosa	0.9	0.2	0.4			0.4													
Trifarina bradyi																	0.4		
Uvigerina canariensis	2.4	0.2	1.9	0.4	0.6	1.5	1.1	1.3	2.7	0.5	0.4		0.2		0.2			0.5	

Appendix 4-1. (continued)

species \ depth(cm)	200	210	220	230	240	250	260	270	280	300	320	340	360	380	400	420	460	480	510
Uvigerina dirupta																			
Virgulopsis orientalis									0.4	0 2							0 4		
Astrononion tasmanensis	2.0	2 7	1 1		2.5	1.9	2.4	2.7	2 7	0 5	3 4	0.3	0 4	0 2	0.2	0.6	1 3		
Cribrononion incertum					0.3		0.4	0 3								2.4			
Cribrononion parisuturalis		0.7										1 3			0 7		0.4	0.5	
Cribrononion subincertum	0.2	2.9	0.4	3.0	1 0		2 2	1 0	0 6	1.2	6 0	2.6	2.4	4 3	2 6	2 7	1 3	1.9	2 6
Cribrononion sp.					0.6					0 5		0 6	0.4	0.5			0 4		
Elphidiella Kiangsuensis				0.4		0.4	0 2			1.0		0.6	0.9		0 7				
Elphidium advenum	6.8	4.7	6.8	5.6	5 4	8 7	7 2	12.0	5.1	6.4	6.4	8 7	9 2	7 5	8 2	10.3	13.8	12.3	8.7
Elphidium crispum																			1.7
Elphidium magellanicum	4.1	30.4	15 4	24.1	17 8	8.0	20 2	8.7	9.8	24 2	20 9	24.8	35.5	43.2	39.6	39.8	31 3	37.0	29 6
Florilus decorus	1 1	1.1	1.1	1 1	1.9	1.9	0.7	1 3	1.1	1 2	0.4	1 3	1 1	1 6	2.1	2.1	2 9	3 3	1.7
Melonis sp.														0.2					
Nonion akitaense						1 1	1.3	0.3		0.2		0.3							
Nonion stella				0.4		0 8	0.2	0.3											
Nonion sp.																	0 4		
Nonionella jacksonensis	1.1	0 2	0 4		0.3				0.6										
Nonionella magnalingua																			
Nonionella sp.	0 2	0 4			0 3			0 3	0 1			0.3							
Protelphidium compressum		0 4			0.3	1.1		0.3	0.4	1.2	0 9	0 6	1 5	0.9		0.6	0 4		
Pseudononionella sp.												1.3	0 2	0 2					
Pullenia bulloides											0 4								
Pullenia quinqueloba			0 8		0.3		0.2		0.1				0.2		0.2				
Spirilina sp.																			
Stomoloculina multangula				0 8								0 3			0 2		0.4	0.5	0.9
Ammonia annectens									0 1										
Ammonia compressiuscula	2.6	1 8	1 9	0 8	2.9	1.5	2 6	1.7	3.2	0 5	4 7	1 3	0 4	1 6	0.2	0.3	0.8	0.9	0.9
Ammonia confertitesta		3.4	4.1		0 3	15 2	14.3	16.7	6.6	17.8	15.0	16.1	15.1	15 0	14.0	10.6	4 6	6 6	6.1
Ammonia convexdorsa	0.9	2.0		2.6	0.6	0 8	1 5	0.3	0.1	0.7	2.1	2.3	1 1	0.5	0 7	0.9	0.4	1 4	2.6
Ammonia ketienziensis angulata	3 1	1.3	1.5	2.3	2.5	0.8	2 0	3.3	4.4	1.0	1.3	1.0			0.2		1 7		1.7
Ammonia limbatobeccarii	0 7	1 1	0 8	0.4	0.3	2 3		0.7			2.1		0.4	0 2	0.2	0.3			

Appendix 4-1. (continued)

species \ depth(cm)	200	210	220	230	240	250	260	270	280	300	320	340	360	380	400	420	460	480	510
Ammonia multicella									0.3										
Ammonia pauciloculata	10.9	2.2	6.4	4.5	9.6	5.7	3.5	6.7	9.0	2.4	0.4	1.0	0.4		0.2	0.3	2.5		3.5
Ammonia tepida	0.2		1.5	1.9	1.0	0.4					0.4	1.3							
Buccella frigida	2.2	2.5	1.5	1.5	0.3	3.4	1.5	0.7	0.3	1.5	1.7	1.0	2.4	3.6	4.0	3.3	2.1	0.5	3.5
Cancris auriculus	0.7	0.4						0.7	0.1		0.9			0.2					
Cibicides lobatulus	0.4		0.8		0.3		0.7						1.5						
Cibicides pseudoungerianus	0.9	0.4	0.8	1.9	0.6	0.4	0.7	0.3	0.3	1.2	0.4	1.0	0.2	0.5	0.9	0.3	0.4	0.5	
Cibicides sp.		0.7	1.9			1.5	1.3	1.0	2.2	1.2	2.1	3.5	1.1	1.1	3.7	3.3	4.6	2.8	1.7
Cibicidina sp.				0.4	1.0														
Discorbinella bertheloti																		0.5	
Epistominella naraensis	2.2	0.9	5.6	4.1	3.5	2.7	2.9	1.3	2.8	1.7	0.9	1.9	0.7	0.2	0.5	1.2		0.5	1.7
Eponides repandus		0.2											0.7	0.2					
Eponides sp.																			
Gavelinopsis sp.	1.7	1.1	1.5	2.3	0.3	1.1	0.4	1.0	1.7	0.5	0.4		1.3	0.7	0.7	0.3			0.9
Geminospira simaensis				0.4															
Gyroidina nipponica	2.6	0.4	1.5	1.9	1.6	0.8	0.7	0.3	2.1						0.2		2.1		0.9
Gyroidina sp.																			
Hanzawaia nipponica	2.0	0.7	0.8	1.5		0.8	1.3		1.5	1.0	2.1	1.9	1.1	0.5	0.9	2.4	0.4	0.5	0.9
Heterolepa dutemplei	1.7		2.3	2.3	1.0	0.4	0.7	1.3	1.4	1.5	0.9	0.3	1.1	0.5	0.5	0.9			
Hyalinea balthica	1.5		0.4	0.8	1.0	1.1	0.2	0.7	2.0	1.0		0.3							
Hyalinea sp.									0.6										
Lamarkina scabra		0.2																	
Neoeponides procera	0.2					0.4	0.4		0.1						0.2				
Pararotalia nipponica	2.0	3.1	3.8	1.5	2.5	5.3	5.0	7.0	2.1	7.1	10.3	7.4	4.4	3.6	7.5	7.0	7.5	5.2	4.3
Pseudoeponides japonica	0.7				0.3	0.4			0.1			0.3	0.2			0.3	0.4		0.9
Pseudogyroidina sinensis	0.4	0.2	0.8	0.4		0.4	0.4	0.7	0.7		1.3	1.3	0.2	0.9	0.7			0.9	
Pseudorotalia indopacifica					0.3			0.3									0.8	3.3	2.6
Pulsiphonina sp.	0.4		0.4					0.3	0.1					0.2					1.7
Rosalina bradyi			2.6	1.5	1.9	1.5	1.1	0.7	0.4	0.5			1.1	0.5			1.7	0.9	
Rosalina australis	0.7	0.9	0.4	0.4	0.3				0.3	0.2	0.9	0.6	0.9	0.7	1.4			0.9	1.7
Rotalia sp.																			0.9
Sphaeroidina bulloides																			
Seabrookea sp.	0.2								0.1										
counting BF	459	447	266	266	314	264	456	300	712	409	234	310	456	440	429	329	240	211	115

Appendix 4-2. Planktonic foraminifera (larger than 125um) percentages in core 97-02

Species \ Depth (cm)	0	10	20	30	40	50	60	70	80	90	100	110	120	130	140	150	160	170	180	190
Globigerinoides conglobatus		1.5	1.3	0.4	0.5	0.6		0.2	1.0	1.0	1.1	1.3	1.4	0.4						
Globigerinoides ruber	11.3	15.9	15.2	19.8	26.5	22.4	15.1	16.0	21.9	17.3	15.7	14.0	4.1	18.0	7.1	28.6	10.0	16.7	14.3	9.4
Globigerinoides tenellus	7.9	3.5	3.9	5.0	1.4	1.7	3.4	2.2	2.6	3.0	1.1	2.2		0.9	2.0	2.9				4.7
Gs. sacculifer "with sac"					1.4			0.7	1.0		0.7	0.4		0.4				6.3		1.6
Gs. sacculifer "without sac"	5.3	3.5	3.5	1.5	1.4	1.7	10.1	3.7	3.6	3.6	3.3	2.8	4.1	1.6	7.1					
Globigerinella aequilateralis		0.5				1.1		1.0							2.0					
Globigerina calida	23.8	32.3	27.0	24.0	27.4	21.3	10.1	18.7	18.2	13.7	23.0	9.6	26.9	23.2	24.2	14.3	30.0	33.3		29.7
Globigerina bulloides	15.9	10.0	11.7	13.4	12.6	17.8	11.8	15.5	14.1	13.2	6.8	10.0	10.3	13.2	9.1	11.4	10.0			10.9
Globigerina falconensis				0.4							0.4			1.3	1.0					
Bella digitata	2.0	2.5	1.3	0.8	0.5			0.5	0.5	0.5	0.7									
Globigerina rubescens	2.0	1.5	4.5	1.1	0.9	1.1	1.7	0.7	1.0	3.0	2.2	1.3	3.4	1.3		5.6			28.6	3.1
Neogloboquadrina pachyderma L			1.5			1.1	2.5	0.7	3.1	5.1	1.1	5.2	6.9	1.6	5.1					3.1
Neogloboquadrina pachyderma R	0.7		0.9	0.9	1.9	2.3	1.7	1.2	1.0	1.5	1.5	1.7	2.8	1.6	1.0				14.3	
Pulleniatina obliquiloculata	1.3	2.5	4.3	5.7	4.7	2.9	4.2	4.7	3.6	1.5	4.7	10.0	1.4	4.8	4.0	14.3	5.0	8.3	14.3	9.4
Globorotalia inflata					0.5		0.5													
Globorotalia crassaformis		0.5		0.4		0.6														1.6
Globorotalia menardii												0.4				2.9				
Globigerinita glutinata	18.5	12.9	14.8	13.4	8.8	14.9	23.5	21.2	14.1	20.3	22.3	24.5	26.9	21.9	23.2	8.6	30.0	16.7		12.5
Neogloboquadrina dutertrei	9.3	10.4	9.6	12.2	11.2	9.8	13.4	8.2	14.1	10.2	13.1	16.2	10.3	9.2	11.1	8.6	15.0	16.7	28.6	12.5
Globigerina quinqueloba	2.0	2.6	0.9	1.1	0.5	0.6	1.7	2.6		2.0	2.6	0.4	1.4		2.0					
counting PF	151	201	230	262	215	174	119	401	192	197	274	229	145	226	99	35	20	12	7	64

Appendix 4-2.(continued)

Species \ Depth (cm)	200	210	220	230	240	250	260	270	280	300	320	340	360	380	400	420	460	480	510
Globigerinoides conglobatus			10 0																
Globigerinoides ruber	9 1	4 5			12 5		5 3	23 1	11.6			50	16 7					33 3	
Globigerinoides tenellus		4 5			12 5				4 7										
Gs. sacculifer "with sac"					6.3														
Gs sacculifer "without sac"		4 5				5 3		7 7								7 1	5 9		
Globigerinella aequilateralis												50							
Globigerina calida	36 4	36 4	50	50	18.8	21 1	47 4	15 4	27 9	52 9			16 7		100	35 7	17 6		
Globigerina bulloides	27 3	4 5				10 5	5 3	7 7	14.0					50		14 3	17 6		
Globigerina falconensis																			
Bella digitata										5 9									
Globigerina rubescens						10 5				5 9									
Neogloboquadrina pachyderma L		4 5			6 3				2 3	5 9						14 3	5 9		
Neogloboquadrina pachyderma R					6 3					5 9			16 7				5 9		
Pulleniatina obliquiloculata						5 3			4 7										
Globorotalia inflata										5 9									
Globorotalia crassaformis																			
Globorotalia menardii																			
Globigerinita glutinata	9 1	18.2	10.0	50	18 8	31 6	21 1	7 7	18 6	5 9	33 3		33.3	50			23 5	33 3	100
Neogloboquadrina dutertrei	18 2	22 7	30 0		18 8	15 8	21 1	38 5	16 3	11 8	66 7		16 7			28 6	23 5	33 3	
Globigerina quinqueloba																			
counting PF	11	22	10	2	16	19	19	13	43	17	3	2	6	2	3	14	17	3	1

Appendix 4-3. PF/(BF+PF) ratio, foraminiferal abundances, BF diversity [S, H(S)], BF assemblages and coarse fraction (CF, >0.063mm) in the sediment

depth (cm)	PF/PF+BF (%)	PF abundance per gram	BF abundance per gram	S	BF H(S)	agglutinated (%)	porcelaneous (%)	Lagenids (%)	serial (%)	planispiral (%)	trochospiral (%)	CF (%)
0	43.49	7904	10272	39	2.75	0.0	1.9	1.9	46.4	10.3	39.6	7.2
10	36.09	10860	19264	42	2.70	1.3	3.2	2.0	45.5	7.6	40.4	9.2
20	30.69	5200	11744	43	2.78	1.4	4.9	1.9	47.5	9.1	35.1	13
30	27.47	5120	13520	50	2.68	2.8	2.8	1.1	48.3	9.3	35.5	18.4
40	28.13	6976	17824	53	2.59	2.4	3.5	1.2	48.3	7.6	37.0	14.4
50	29.72	4560	10784	44	2.74	2.2	3.3	1.5	48.4	7.4	37.2	18.3
60	26.15	1640	4632	42	2.71	2.1	4.5	1.9	51.5	9.2	30.9	28.1
70	24.94	2293	6901	49	2.62	1.8	3.9	1.3	46.5	8.2	38.4	29.5
80	23.53	2347	7627	44	2.73	2.5	5.9	1.3	46.4	10.2	31.7	41.9
90	30.71	2752	6208	49	2.83	2.9	4.8	2.4	47.6	8.9	33.2	49.8
100	28.73	1355	3360	48	2.73	3.5	4.8	2.9	44.3	11.1	33.5	50.4
110	36.54	1520	2640	55	3.18	2.6	8.5	2.0	34.1	9.1	43.6	55.4
120	41.41	784	1109	50	3.20	4.1	8.2	1.9	37.3	8.9	39.7	59.6
130	40.66	755	1101	50	3.27	3.9	10.9	4.4	31.5	16.0	33.2	61.9
140	39.00	624	976	52	3.36	2.5	11.5	2.5	29.5	12.8	41.0	60.4
150	29.41	120	288	44	3.15	4.2	8.8	1.9	30.6	20.8	33.8	38.4
160	12.66	32	221	61	3.09	2.2	8.9	1.8	35.5	14.7	37.0	27.7
170	11.55	22	168	53	3.03	1.9	13.1	2.1	33.0	18.8	31.1	23.7
180	17.05	24	117	44	3.15	1.0	9.9	2.1	28.4	26.4	32.2	46.7

Appendix 4-3. (continued)

depth (cm)	PF/PF+BF (%)	PF abundance per gram	BF abundance per gram	S	BF H(S)	agulitinated (%)	porcelaneous (%)	Lagenids (%)	serial (%)	planispiral (%)	trochospiral (%)	CF (%)
190	44 74	293	362	57	3.59	6.2	10 8	3.3	20 1	19.9	39.4	27 8
200	37 72	111	184	60	3.25	2.6	8.3	3.7	31 2	15.5	38.6	14 5
210	14 53	30	179	49	2.88	1.3	20.1	1 6	9.6	43.6	23.7	29 6
220	13 36	16	106	52	3.31	1.1	6.8	3 4	21.8	25.9	41.0	14 2
230	9.83	12	106	47	3.06	1.5	10.9	3.8	15.4	35.3	33 1	12
240	21.11	34	126	54	3.17	1.3	11.5	4.8	19.4	30.9	32.2	74 7
250	20 00	17	66	46	3.27	1.1	8.0	2.3	18.2	23.9	46.6	81
280	18.43	26	114	50	3 06	0.4	5.3	1.5	16.4	35.1	41.2	39 6
270	15.49	14	75	51	3.14	1 1	7 7	3.3	17.9	20.4	49.6	72 8
280	22.69	52	178	57	3.25	1.4	4 9	1 4	28.9	20.5	42.7	69 5
300	10.11	12	102	48	2.83	0.7	8.3	1 2	13 4	36.4	39 9	70 2
320	3 70	1	29	38	2.87	0.9	7.7	0.0	5.1	38.5	47.9	64
340	8.28	4	39	43	2.94	1.0	5 5	2.6	5.2	43.2	42.8	37
360	11 11	7	57	46	2 54	0.9	5.7	1.5	5.5	52.0	34 4	71 2
380	11.82	7	55	41	2.35	0 0	3.2	3.2	4.3	58.6	30 7	70.3
400	10.06	6	54	37	2.29	0 0	5 6	1.2	1.9	54.5	36 8	58.9
420	6.53	6	82	33	2.42	1 5	2 4	2.4	3.3	58.7	31 6	52.9
460	11.78	3	20	37	2.72	1.3	6 7	1 7	7 9	52.5	30 0	93 5
480	3.65	1	18	38	2.52	0.0	10.4	1 4	7 1	55.5	25 6	96 1
510	8.73	1	10	37	2.67	1 7	8.7	1 7	6 1	45 2	36.5	93 6